



AMERICAN UNIVERSITY OF BEIRUT

PREDICTING STEADY TWO-PHASE FLOW OF REFRIGERANTS  
UNDER VARIABLE HEAT FLUX

BY  
MOHAMAD MAJED HACHEM

A thesis  
submitted in partial fulfillment of the requirements  
for the degree of Master of Engineering  
to the Department of Mechanical Engineering  
of the Faculty of Engineering and Architecture  
at the American University of Beirut

Beirut, Lebanon  
JANUARY 2020

AMERICAN UNIVERSITY OF BEIRUT

PREDICTING STEADY TWO-PHASE FLOW OF  
REFRIGERANTS UNDER VARIABLE HEAT FLUX

by  
MOHAMAD MAJED HACHEM

Approved by:

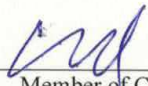
\_\_\_\_\_  
Dr. Fadl Moukalled, Professor  
Department of Mechanical Engineering, AUB

  
Advisor

\_\_\_\_\_  
Dr. Marwan Darwish, Professor  
Department of Mechanical Engineering, AUB

  
Member of Committee

\_\_\_\_\_  
Dr. Kamel Aboughali, Professor  
Department of Mechanical Engineering, AUB

  
Member of Committee

\_\_\_\_\_  
Dr. Iyad Faissal, Assistant Professor  
Department of Mechanical Engineering, RHU

  
Co-Advisor

Date of thesis defense: January 8, 2020

AMERICAN UNIVERSITY OF BEIRUT  
THESIS, DISSERTATION, PROJECT RELEASE FORM

Student Name: Hachem Mohamad Majed  
Last First Middle

Master's Thesis  Master's Project  Doctoral Dissertation

I authorize the American University of Beirut to: (a) reproduce hard or electronic copies of my thesis, dissertation, or project; (b) include such copies in the archives and digital repositories of the University; and (c) make freely available such copies to third parties for research or educational purposes.

I authorize the American University of Beirut, to: (a) reproduce hard or electronic copies of it; (b) include such copies in the archives and digital repositories of the University; and (c) make freely available such copies to third parties for research or educational purposes after: **One** ~~year~~ **year from the date of submission of my thesis, dissertation, or project.**  
**Two** ~~years~~ **years from the date of submission of my thesis, dissertation, or project.**  
**Three** ~~years~~ **years from the date of submission of my thesis, dissertation, or project.**

Ahachem

Signature

Date

## ACKNOWLEDGMENTS

I would first like to thank my thesis advisor Dr. FadlMoukalled for his encouragement and support during my study at AUB. The door to his office was always open whenever I ran into a trouble spot or had a question about my research or writing. His kindness and thoughtful considerations were the main factors helping me to continue my Master's degree after a three-year disconnection period.

My recognition and gratitude are also addressed to Dr. IyadFaissal who offered his private time and unconditional support during days and nights of the last year and helped in breaking obstacles that I encountered.

I would also like to acknowledge Dr. Marwan Darwish and Dr. KamelAoughali, for their attendance and valuable comments which enriched the content of my work.

Finally, I express great thanks to my family (Father, Mother, and my wife) for their patience and continuous unconditional support.

# AN ABSTRACT OF THE THESIS OF

Mohamad MajedHachem for Master of Engineering

Major: Mechanical Engineering

Title: Predicting Steady Two-Phase Flow of Refrigerants under Variable Heat Flux

Two phase flow of refrigerants during evaporation and condensation subjected to variable heat flux is being studied. Several types of refrigerants (R134a, R12, R22, R32 and R143a) are being studied as the internal fluid of the heat exchanger with major emphasis on R134a while water is assumed to be the outer fluid. Parallel and counter flows are both being studied where results show the favorability of parallel flow heat exchangers over counter flow heat exchangers unlike the results of single phase heat exchangers. Numerical analysis of refrigerant flow is investigated using finite volume method where both thermodynamic and hydrodynamic refrigerants properties are being calculated and checked at each control volume to assure convergence of iterations. Axial heat conduction through the inner pipe is being studied for constant heat flux and variable heat flux. Results have shown that neglecting the significance of axial heat conduction where constant heat flux is applied could over predict the heat exchanger size while under predict it in the variable heat flux case.

# CONTENTS

ACKNOWLEDGEMENTS.....	v
ABSTRACT.....	vi
LIST OF ILLUSTRATIONS.....	x
LIST OF TABLES.....	xii

## Chapter

I. INTRODUCTION.....	1
II. THERMODYNAMIC & TRANSPORT PROPERTIES OF REFRIGERANTS.....	6
A. R134a Equation of State.....	6
1. R134a Helmholtz free energy .....	7
a. R134a Ancillary Equations .....	7
b R134a Ideal Dimensionless Helmholtz Free Energy .....	9
c. R134a Residual Dimensionless Helmholtz Free Energy .....	9
d. R134a First and Second Derivatives of Dimensionless Helmholtz Free Energy ....	10
e. Thermodynamic Properties of R134a .....	11
B. Dynamic Viscosity of R134a .....	12
C. Thermal Conductivity of R134a.....	15
D. Surface Tension of R134a.....	17
III. CONSTANT HEAT FLUX - NO AXIAL HEAT CONDUCTION SOLUTION METHODOLOGY & RESULTS .....	18
A. Mathematical Model.....	18
1. Continuity Equation .....	19
2. Energy Equation.....	20
3. Momentum Equation .....	20

a. Wall Shear Stress Calculation.....	20
B. Equations Discretization.....	21
1. Continuity Equation.....	21
a. Vapor Continuity Equation.....	21
b. Liquid Continuity Equation.....	22
2. Energy Equation.....	22
a. Wall Temperature.....	22
3. Momentum Equation.....	23
C. Solution Algorithm.....	23
D. Solution Flow Chart.....	25
E. Results.....	26
IV. VARIABLE HEAT FLUX - NO AXIAL HEAT CONDUCTIONSOLUTION METHODOLOGY & RESULTS.....	32
A. Mathematical Model.....	32
B. Solution Method for Parallel Flow.....	34
C. Solution Method for Counter Flow.....	35
D. Solution Flow Chart.....	37
E. Results.....	38
V. CONSTANT HEAT FLUX - AXIAL HEAT CONDUCTIONSOLUTION METHODOLOGY & RESULTS.....	41
A. Mathematical Model.....	41
B. Solution Method.....	42
1. Pipe Wall Energy Equation.....	42
C. Solution Flow Chart.....	44
D. Results.....	45
VI. VARIABLE HEAT FLUX - AXIAL HEAT CONDUCTION SOLUTION METHODOLOGY & RESULTS.....	47



A. Mathematical Model.....	47
B. Solution Method.....	48
C. Solution Flow Chart.....	49
D. Results.....	50
VII. PARAMETRIC STUDY.....	52
E. Effect of Refrigerant Type.....	52
F. Effect of Variation of Pipe Diameter at Constant Mass Flux.....	55
G. Effect of Outer Fluid Flow Direction.....	56
VIII. CONCLUSION & FUTURE WORK.....	60
IX. REFERENCES.....	61

## ILLUSTRATIONS

Figure	Page
1. Comparison of P-T diagram between Refprop and Matlab .....	8
2. Comparison of Density-Temp diagrams between Refprop and Matlab .....	9
3. Liquid and Vapor Cv and Cp curves w.r.t Pressure.....	12
4. Comparison of Liquid and Vapor viscosities generated by Refprop and Matlab.....	15
5. Comparison of Liquid and Thermal Conductivities between Refprop and Matlab.....	17
6. Comparison of Surface Tension between Refprop and Matlab .....	18
7. Cross section of heat exchanger pipe.....	19
8. Variation of pressure, refrigerant and heat exchanger wall temperature, enthalpy, flow quality, volume fraction of R12 during evaporation subjected to Constant Heat Flux .....	27
9: Variation of heat transfer coefficient, liquid velocity, and vapor velocity of R12 during evaporation .....	28
10: Variation of pressure, refrigerant and heat exchanger wall temperature, enthalpy, flow quality, volume fraction of R12 during condensation .....	30
11: Variation of heat transfer coefficient, liquid velocity, and vapor velocity of R12 during condensation.....	30
12. Variation of pressure, refrigerant and heat exchanger wall temperature, heat transfer coefficient, flow quality, of R134a during evaporation .....	31
13. Cross section of concentric pipe .....	32
14. Dimensions of inner and outer pipe in concentric pipe .....	33
15. Variation of pressure, refrigerant and heat exchanger wall temperature, water temperature, heat transfer coefficient, and flow quality of R134a during evaporation subjected to variable heat flux, parallel.....	38

16. Variation of pressure, refrigerant and heat exchanger wall temperature, water temperature, heat transfer coefficient, and flow quality of R134a during evaporation subjected to variable heat flux, counter flow .....	39
17. Cross section of evaporator pipe.....	41
18. Section showing pipe wall grid.....	42
19. Variation of pressure, refrigerant and heat exchanger wall temperature, heat transfer coefficient, flow quality, of R134a during evaporation with axial heat conduction taken into consideration .....	45
20. Cross section of concentric pipe .....	47
21. Variation of pressure, refrigerant and heat exchanger wall temperature, heat transfer coefficient, flow quality, of R134a during evaporation with axial heat conduction taken into consideration .....	50
22. Variation of pressure, refrigerant and heat exchanger wall temperature, heat transfer coefficient, flow quality, during evaporation of R143a, R22, R32, R134a and R12. ....	53
23. Flow quality variation vs pipe length in the 3 case. $D_i=5\text{cm}$ , $D_i=10\text{cm}$ , and $D_i=15\text{cm}$ ...	56
24. Variation of pressure, refrigerant and heat exchanger wall temperature, heat transfer coefficient, flow quality, during evaporation of R134a for $D_i=5\text{c}$ , $D_i=10\text{cm}$ , and $D_i=15\text{cm}$ .	57
25. Variation of pressure, refrigerant and heat exchanger wall temperature, heat transfer coefficient, flow quality, during evaporation of R134a for parallel flow and counter flow of water .....	58

## TABLES

Table	Page
1. Coefficients and exponents of R134a residual part of Helmholtz equation of state.....	10
2. Coefficients used to calculate reduced effective collision cross section .....	13
3. Parameters used to solve for 2nd viscosity virial coefficient.....	13
4. Parameters used to calculate Higher density terms.....	14
5. Parametric study showing effect of axial heat conduction on evaporator length during constant heat flux .....	46
6. Parametric study showing effect of axial heat conduction when refrigerant mass flux is varied on evaporator length during variable heat flux, $G_w=114\text{kg/m}^2\text{s}$ .....	51
7. Parametric study showing effect of axial heat conduction when water mass flux is varied on evaporator length during variable heat flux, $G_r=400\text{kg/m}^2\text{s}$ .....	51
8. Length, average wall heat flux, pressure drop, refrigerant temp drop and water temp drop for R12, R134a, R143a, R22 & R32 respectively with $G_r 350\text{kg/m}^2\text{s}$ .....	54
9. Length, average wall heat flux, pressure drop, refrigerant temp drop and water temp drop for R12, R134a, R143a, R22 & R32 respectively with $G_r 250\text{kg/m}^2\text{s}$ .....	55

# CHAPTER I

## INTRODUCTION

The huge increase in energy consumption in the last decade, and the fact that a great portion of this energy is consumed by residential buildings especially in HVAC systems, has led to an intensive interest in improving the efficiency of air conditioning systems. This can be done via enhancing the efficiency of each component constituting the refrigeration system. [1, 2] pointed out the relatively easy task of understanding the dynamics of both expansion valves and compressors compared to that of evaporators and condensers. This is the reason the literature is filled with heat exchanger modeling approaches. Thus predicting the performance of evaporators' and condensers' coils, by analyzing the two-phase flow regimes in them, is of much interest to manufacturers and researchers.

Heat exchangers efficiency is intensively studied and several papers addressed this topic using one or more of the following 3 ways.

- Using Empirical and theoretical formulas
- Using experimental investigation
- Using numerical techniques

Fayssal and Moukalled [3] studied steady two phase flow of refrigerants in evaporators and condensers under constant heat flux. [3] results show that using a multi-pipe heat exchanger is more efficient than a single-pipe as long as both of them provide same mass flow rate of refrigerant. Moo-Yeon Lee [4] studied the performance of a two parallel refrigeration cycles for a special purpose vehicle. According to [4], as refrigerant charge decreases, coefficient of

performance COP of system increases due to the decrease in compressor's work. In their study of inverter split type air-conditioner, N. Rachapradit et al [5] varied refrigerant mass flow rates, air volume flow rates, and set point temperatures to study their effect on cooling capacity, power consumption, COP, and sensible heat ratio SHR. [5] concluded that increasing air volume flow rate increases both cooling capacity and COP while increasing refrigerant mass flow rate increases cooling capacity and decreases COP due to more power consumption by compressor. D. Parker et al [6] investigated experimentally the impact of evaporator coil airflow in residential air-conditioning systems. [6] found that a 25% reduction in the airflow (from 400cfm to 300cfm per ton) decreases both energy efficiency ratio EER and SHR. A further decrease to less than 200 cfm per ton increases the possibility of ice formation on coil tubes. A. Ebrahimi-Mamaghani et al [7] assessed dynamics of two phase flow in vertical pipes. They showed that choosing an optimal flow velocity enhances the stability of the system. Z. Baniamerian et al [8] proposed a new analytical model for studying thermal and fluid characteristics of annular two phase flow. The proposed model took into consideration each of the following mass transfer phenomenon: entrainment, evaporation, deposition and condensation. T. Okawa et al [9] carried out experiments showing that liquid film thickness in annular two-phase flow subjected to flow oscillations decreases as oscillation period increases.

Heat transfer coefficient used in this study will have a major effect on heat transfer on both sides of the pipe, either from refrigerant-pipe side or from outer fluid-pipe side. Sieder-Tate [10] correlation for Nusselt number calculation is dependent on Reynolds and Prandtl numbers in addition to the dynamic viscosities ratio at mean bulk temperature to wall temperature. S. Whitaker [11] proposed a modification of [10] correlation where the constants differ. Another popular heat transfer correlation, for turbulent flow in a pipe, is that of Gnielinski [12] where

Nusslet number is calculated dependent on Prandtl and Reynolds numbers in addition to Darcy friction factor. I.Tosun [13] evaluated the above mentioned heat transfer correlations, including one of the simplest correlations for convective heat transfer coefficient for turbulent flow inside a pipe that is Dittus-Boelter correlation [14] where Nusselt number calculation depends on Reynolds and Prandtl numbers only.

[11] also correlated Nusselt number for flow normal to a single cylinder using same parameters but with different constants. From such a correlation, the heat transfer coefficient is to be determined. Zhukauskas [15] proposed, for flow normal to a single cylinder, a correlation dependent on Reynolds number, and Prandtl number at 3 locations (Prandtl at desired temperature, Prandtl at reference temperature, and Prandtl at pipe wall temperature). Churchill-Bernstein [16] correlation is commonly used for cross flow over a cylinder. The main difference is that all properties are evaluated at film temperature rather than outer fluid temperature.

Several researchers [3, 8, 17-22] studied certain aspects in two phase flow of refrigerants subjected to uniform heat flux on the pipe wall. However, the heat transfer coefficient depends mainly on fluid flow and thus heat flux doesn't have a fixed value. It varies along the pipe, even in steady state conditions.

It is quite hard to develop or mimic the same experimental conditions previously studied by researchers so we will use numerical methods to predict the two phase flow of refrigerants in heat exchangers. Using numerical techniques, the effect of modifying the input heat flux (by modifying either outer fluid temperature or speed), refrigerant type, pipe diameter... can be studied. This flexibility is only provided by numerical techniques and this will aid in the design process of heat exchangers. Another advantage of numerical techniques is the possibility of

knowing a wide of set of variables at any point in the domain being studied that is whole-flow field data.

This study predicts the behavior of pure refrigerants exposed to constant and variable heat flux in evaporators and condensers, which are modeled as horizontal circular pipes. It will enhance the design process of heat exchangers by optimizing the length of coil used in evaporators and condensers.

Axial heat conduction through evaporator inner pipe is neglected in most simulations. Some researchers studied the effect of axial heat conduction in single phase flow. F. Moukalled et al [23] studied the effect of axial heat conduction in a longitudinally externally finned pipe. The flow was a turbulent-convection single phase flow. Results of [23] have shown that as thermal conductivity of pipe wall increases, the heat transfer rate to the fluid increases. On the other hand, especially for mini channels, axial heat conduction could lead to a loss in efficiency as G. Maranzana et al [24] found.

Celata[25] concluded in his review that till now, contradictions between theoretical and experimental studies of the effect of axial heat conduction in micro and mini channels exist. Most researchers assume nucleate boiling is the dominant mode of heat transfer in two phase flow. To the best of our knowledge, no study of axial heat conduction effect of annular two phase flow solely is present in the literature.

The annular flow is considered to be the dominating flow regime of the mixture during the change-of-phase process. Fayssal and Moukalled [3] studied steady two phase flow of refrigerants in evaporators and condensers under constant heat flux neglecting the effect of axial conduction through the pipe. This work extends the study of [3] by considering variable heat flux



and different outer fluid flow configurations around the pipe in addition to studying the effect of axial heat conduction through the pipe. Refrigerant flow will be assumed as steady one dimensional flow while outer fluid flow through evaporator will be assumed to be either parallel, or counter flow. Parametric analysis of refrigerant type, outer fluid mass flow rate, refrigerant mass flow rate, and coil pipe diameter will be investigated.

Ban of use of ozone depleting refrigerants like CFCs and HCFCs took its first step at the Montreal protocol in 1987. Dichlorodifluoromethane (R-12), a CFC refrigerant typically used in HVAC industry, was replaced in most HVAC systems by R134a, a hydrofluorocarbon HFC of lower global warming potential and insignificant ozone depleting potential compared to R12 [26]. After European Union directive 2006/40/EC banned the use of car AC refrigerants of global warming potential higher than 150 [27], the R1234yf hydrofluoroolefins (HFO) was proposed in many studies, one of them by T. Mahajani<sup>1</sup> and P. Lokhande [28], as an alternative refrigerant for R134a in automotive air conditioning systems due to its low global warming effect compared to that of R134A which is 1300. In spite of this fact, the use of R1234yf isn't popular enough and most appliances still depend mainly on R134a. Also due to the lack of information, especially from scientific papers, we couldn't have saturation tables of transport and thermodynamic properties of R1234yf. These two reasons prevented us from studying R1234yf as one of the refrigerants in our parametric study.

As we mentioned earlier several types of refrigerants will be studied including R12, R22, R32, R143a, and R134a. R134A will be taken as a reference in other parametric studies (pipe diameter, outer fluid speed, tube roughness...). Two phase flow of R134a subjected to heat transfer either with air or water will be investigated where length needed for R134a to totally evaporate is to be determined during the numerical analysis.

## CHAPTER II

# THERMODYNAMIC & TRANSPORT PROPERTIES OF REFRIGERANTS

### A. R134a Equation of State

R134a will be used as the base refrigerant. [3] used Refprop to get the thermodynamic properties of refrigerants. In our study, a Matlab code will be used to solve for the evaporation and condensation of the refrigerant in the heat exchanger. The link between Matlab and Refprop is needed at each control volume, and this link is time and memory-consuming. Thus, thermodynamic properties of refrigerants used in our study will be calculated in Matlab using the equation of state of each refrigerant.

In order to solve for R134a thermodynamic properties at each control volume, R. Tillner-Roth and H. Baehr [29] equation of state for R134a was used, given saturation pressure, to find temperature, liquid and vapor entropies, liquid and vapor enthalpies, liquid and vapor densities, liquid and vapor specific heat at constant pressure  $C_p$  and specific heat at constant volume  $C_v$ .

M.L. Huber et al [30], R.A. Perkins et al [31], and McLinden et al [32] works were used to calculate R134a viscosities and thermal conductivities for liquid and vapor phases respectively.

Surface tension was calculated using A. Mulero et al [33], and M. Okada and Y. Higashi [34] works. Note that, these mentioned references were used by Refprop software engine to calculate R134a thermodynamic properties and, for the purpose of comparing Matlab calculations with those of Refprop, we used them.

### ***1.R134a Helmholtz free energy***

Helmholtz free energy is a thermodynamic potential that measures the useful work obtainable from a closed thermodynamic system at a constant temperature and volume (isothermal, isochoric). The Helmholtz energy is defined as:  $A=U-TS$

Dimensionless Helmholtz free energy  $\Phi$  is used in calculating refrigerant's thermodynamic

properties.  $\Phi(\tau, \delta) = \frac{A}{RT} = \Phi^{\circ}(\tau, \delta) + \Phi^r(\tau, \delta)$  eq. 2-1

Where  $R = \frac{R_m}{M}$  is the gas constant of HFC-134a

$R_m = 8.314471 \text{ J/mol.K}$  and Molar mass  $M = 0.102032 \text{ Kg/mol}$

$\tau = \frac{T_c}{T}$  is the inverse reduced temperature where  $T_c = 374.18$

$\delta = \frac{\rho}{\rho_c}$  is the reduced density where  $\rho_c = 508 \text{ kg/m}^3$

The dimensionless form  $\Phi$  of the fundamental equation of state is split into an ideal part  $\Phi^{\circ}$  describing ideal gas properties and into a residual part  $\Phi^r$  taking into account the behavior of the real fluid.

#### a.R134a Ancillary Equations

As will be stated later the sole variable known at each control volume will be Pressure thus ancillary equations relating pressure to temperature and density were provided by R. Tillner-Roth and H. Baehr [26].

Saturated Vapor Pressure P (MPa):

$$\vartheta \ln \frac{P}{P_c} = -7.686556 \theta + 2.311791 \theta^{\frac{3}{2}} - 2.039554 \theta^2 - 3.583758 \theta^4 \text{ eq. 2-2}$$

Where:  $\vartheta = \frac{T}{T_c}$ ,  $\theta = 1 - \vartheta$  and  $P_c = 4.05629 \text{ Mpa}$

Figure 1 shows good agreement between Refprop generated curve and that of Matlab.

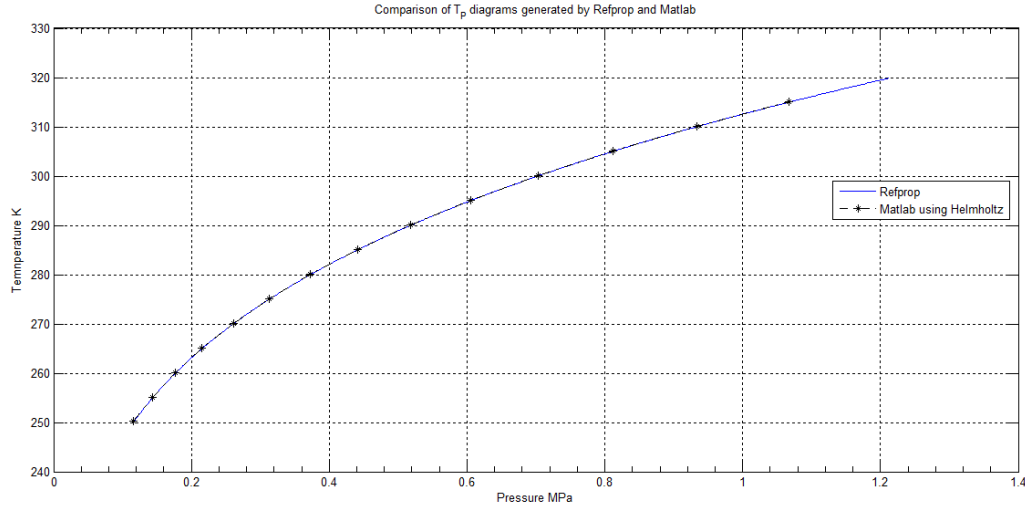


**Figure 1: Comparison of P-T diagram between Refprop and Matlab**

Saturated Liquid Density  $\rho'$  ( $\frac{kg}{m^3}$ ):

$$\rho' = 518.20 + 884.13 \theta^{\frac{1}{3}} + 485.84 \theta^{\frac{2}{3}} + 193.29 \theta^{\frac{10}{3}} \text{ eq. 2-3}$$

Saturated Vapor Density  $\rho''$  ( $\frac{kg}{m^3}$ ):

$$\begin{aligned} \ln \frac{\rho''}{\rho^0} = & -2.837294 \theta^{\frac{1}{3}} - 7.875988 \theta^{\frac{2}{3}} + 4.478586 \theta^{\frac{1}{2}} - \\ & 14.140125 \theta^{\frac{9}{4}} - 52.361297 \theta^{\frac{11}{2}} \text{ eq. 2-4} \end{aligned}$$

Where  $\rho^0 = 516.86 \text{ kg/m}^3$

Figure 2 shows also good agreement between saturated liquid and vapor densities of Refprop and Matlab respectively.

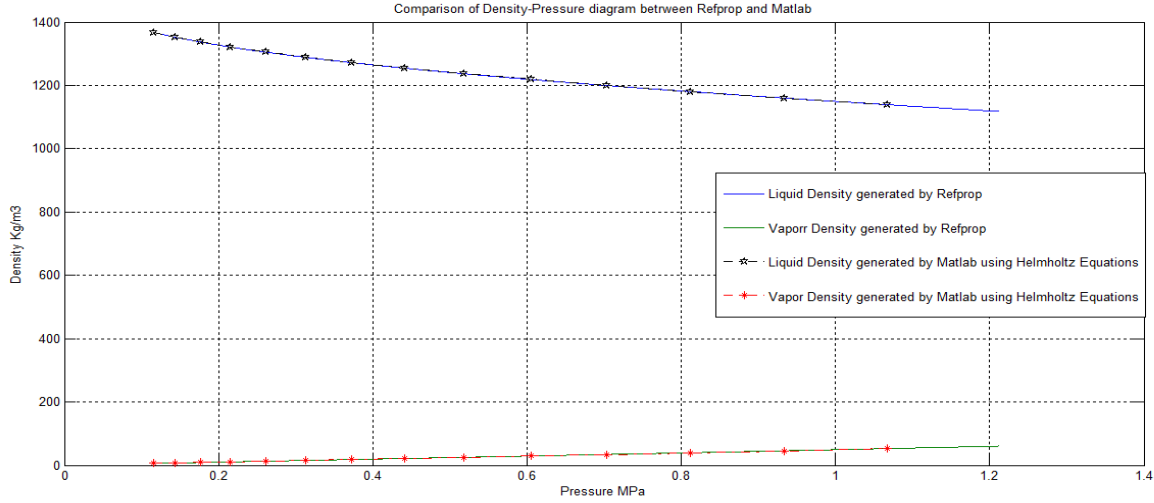


Figure 2: Comparison of Density-Temp diagrams between Refprop and Matlab

### b R134a Ideal Dimensionless Helmholtz Free Energy

The ideal dimensionless Helmholtz energy is defined as:

$$\Phi^o(\tau, \delta) = a_1^o + a_2^o \tau + a_3^o \ln \tau + \ln \delta + a_4^o \tau^{-1/2} + a_5^o \tau^{-3/4} \text{eq. 2-5}$$

Where:

$$a_1^o = -1.019535, a_2^o = 9.047135, a_3^o = -1.629789, a_4^o = -9.723916, \text{ and } a_5^o = -3.927170$$

To calculate  $\Phi^o(\tau, \delta)$ , the two unknown are temperature and density (liquid or vapor) which can be known from ancillary equations stated above.

### c. R134a Residual Dimensionless Helmholtz Free Energy

The residual dimensionless Helmholtz energy is defined as:

$$\Phi^r(\tau, \delta) = \sum_{i=1}^8 a_i \tau^{t_i} \delta^{d_i} + \exp(-\delta) \sum_{i=9}^{11} a_i \tau^{t_i} \delta^{d_i} + \exp(-\delta^2) \sum_{i=12}^{17} a_i \tau^{t_i} \delta^{d_i} + \exp(-\delta^3) \sum_{i=18}^{20} a_i \tau^{t_i} \delta^{d_i} + a_{21} \exp(-\delta^4) \tau^{t_{21}} \delta^{d_{21}} \text{eq. 2-6}$$

Where the coefficients used are listed in table 1

**Table 1: Coefficients and exponents of R134a residual part of Helmholtz equation of state**

i	a <sub>i</sub>	t <sub>i</sub>	d <sub>i</sub>	i	a <sub>i</sub>	t <sub>i</sub>	d <sub>i</sub>
1	0.05586817	-0.5	2	12	0.0001017263	1	4
2	0.498223	0	1	13	-0.5184567	5	1
3	0.02458698	0	3	14	-0.08692288	5	4
4	0.0008570145	0	6	15	0.2057144	6	1
5	0.0004788584	1.5	6	16	-0.005000457	10	2
6	-1.800808	1.5	1	17	0.0004603262	10	4
7	0.2671641	2	1	18	-0.003497836	10	1
8	-0.04781652	2	2	19	0.006995038	18	5
9	0.01423987	1	5	20	-0.01452184	22	3
10	0.3324062	3	2	21	-0.0001285458	50	10
11	-0.007485907	5	2				

#### d. R134a First and Second Derivatives of Dimensionless Helmholtz Free Energy

First and second derivatives of both the ideal and residual parts of Helmholtz energy are necessary for solving the thermodynamic properties of R134a. They are calculated using the following relations:

$$\Phi_{\delta}^0 = \frac{1}{\delta} \text{eq. 2-7}$$

$$\Phi_{\tau}^0 = a_2^0 + \frac{a_3^0}{\tau} + \sum_{j=4}^{N^0} a_j^0 t_j^0 \tau^{t_j-1} \text{eq. 2-8}$$

$$\Phi_{\delta}^r = \sum_{i=1}^{N_o} a_i d_i \tau^{t_i} \delta^{d_i-1} +$$

$$\sum_{k=1}^4 (\exp(-\delta^k) \sum_{i=N_{k-1}+1}^{N_k} a_i (d_i - k\delta^k) \tau^{t_i} \delta^{d_i-1}) \text{eq. 2-9}$$

$$\Phi_{\tau}^r = \sum_{i=1}^{N_o} a_i t_i \tau^{t_i-1} \delta^{d_i} + \sum_{k=1}^4 (\exp(-\delta^k) \sum_{i=N_{k-1}+1}^{N_k} a_i t_i \tau^{t_i-1} \delta^{d_i}) \text{eq. 2-10}$$

$$\Phi_{\delta\delta}^0 = \frac{-1}{\delta^2} \text{eq. 2-11}$$

$$\Phi_{\tau\tau}^0 = \frac{-a_3^0}{\tau^2} + \sum_{j=4}^{N^0} a_j^0 t_j^0 (t_j^0 - 1) \tau^{t_j^0-2} \text{eq. 2-12}$$

$$\Phi_{\tau\delta}^0 = 0 \text{eq. 2-13}$$

$$\Phi_{\delta\delta}^r = \sum_{i=1}^{N_o} a_i d_i (d_i - 1) \tau^{t_i} \delta^{d_i-2} +$$

$$\sum_{k=1}^4 (\exp(-\delta^k) \sum_{i=N_{k-1}+1}^{N_k} a_i [d_i^2 - d_i - k\delta^k (2d_i + k - 1 + k\delta^k)] \tau^{t_i} \delta^{d_i-2}) \text{eq. 2-14}$$

$$\Phi_{\tau\tau}^r = \sum_{i=1}^{N_o} a_i t_i (t_i - 1) \tau^{t_i-2} \delta^{d_i} +$$

$$\sum_{k=1}^4 (\exp(-\delta^k) \sum_{i=N_{k-1}+1}^{N_k} a_i t_i (t_i - 1) \tau^{t_i-2} \delta^{d_i}) \text{eq. 2-15}$$

$$\Phi_{\tau\delta}^r = \sum_{i=1}^{N_o} a_i t_i d_i \tau^{t_i-1} \delta^{d_i-1} +$$

$$\sum_{k=1}^4 (\exp(-\delta^k) \sum_{i=N_{k-1}+1}^{N_k} a_i t_i (d_i - k\delta^k) \tau^{t_i-1} \delta^{d_i-1}) \text{eq. 2-16}$$

Abbreviations:

$$\Phi_{\delta} = \left(\frac{\partial\Phi}{\partial\delta}\right)_{\tau} \Phi_{\tau} = \left(\frac{\partial\Phi}{\partial\tau}\right)_{\delta}$$

$$\Phi_{\delta\delta} = \left(\frac{\partial^2\Phi}{\partial\delta^2}\right)_{\tau}$$

$$\Phi_{\delta\tau} = \left(\frac{\partial^2\Phi}{\partial\delta\partial\tau}\right)$$

$$\Phi_{\tau\tau} = \left(\frac{\partial^2\Phi}{\partial\tau^2}\right)_{\delta}$$

e. Thermodynamic Properties of R134a

$$\text{Pressure: } P(\tau, \delta) = RT \rho (1 + \delta \Phi_{\delta}^r) \text{eq. 2-17}$$

$$\text{Enthalpy: } h(\tau, \delta) = RT[1 + \tau (\Phi_\tau^\circ + \Phi_\tau^r) + \delta\Phi_\delta^r] \text{eq. 2-18}$$

$$\text{Isochoric Heat Capacity: } C_v(\tau, \delta) = -R\tau^2(\Phi_{\tau\tau}^\circ + \Phi_{\tau\tau}^r) \text{eq. 2-19}$$

$$\text{Isobaric Heat Capacity: } C_p(\tau, \delta) = C_v + R \frac{(1 + \delta\Phi_\delta^r - \delta\tau\Phi_{\delta\tau}^r)^2}{1 + 2\delta\Phi_\delta^r + \delta^2\Phi_{\delta\delta}^r} \text{eq. 2-20}$$

Good agreement between calculated isobaric and isochoric heat capacities using equation of state with that generated by Refprop is shown clearly in figure 3.

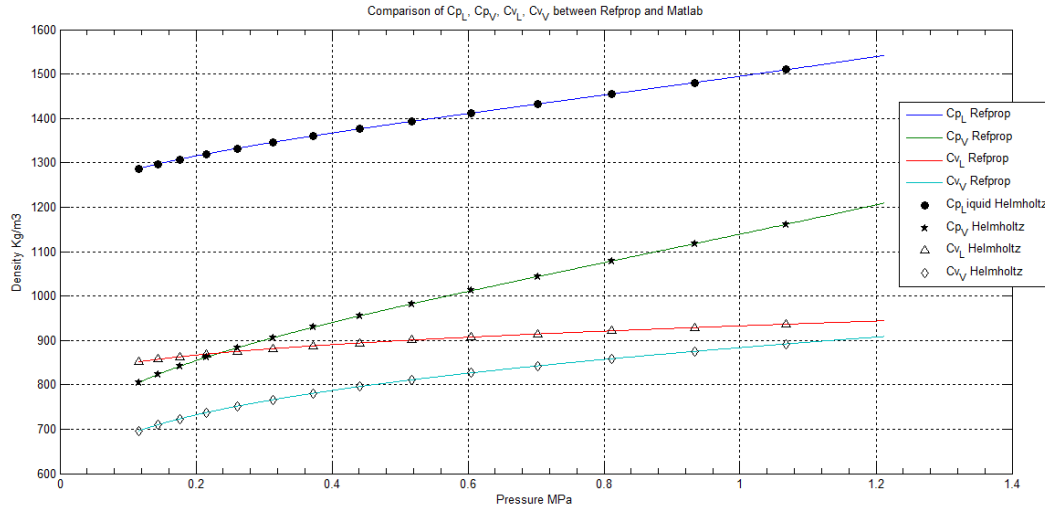


Figure 3: Liquid and Vapor Cv and Cp curves w.r.t Pressure

## B. Dynamic Viscosity of R134a

M.L. Huber et al [30] work is used to calculate R134a liquid and vapor where dynamic viscosity ( $\mu\text{Pa}$ ) of R134a is represented by:

$$\eta(\rho, T) = \eta^*(T)[1 + B_\eta(T)\rho] + \Delta_H\eta(\rho, T) + \Delta_c\eta(\rho, T) \text{eq. 2-21}$$

According to [30], the critical enhancement of viscosity  $\Delta_c\eta(\rho, T)$  is restricted to a region very close to the critical point, and the available viscosity measurements for R134a do not approach the critical region so we set the critical enhancement term to zero.



The ideal viscosity term  $\eta^*(T)$  is calculated using:

$$\eta^*(T) = \frac{0.021 \cdot 357 \sqrt{MT}}{\sigma^2 \vartheta_\eta^*(T^*)} \text{eq. 2-22}$$

Where M is R134a molar mass in kg/m<sup>3</sup>,  $\sigma$  is the length scaling parameter,  $\vartheta_\eta^*$  is the reduced

effective collision cross section calculated by:  $\ln \vartheta_\eta^* = \sum_{i=0}^n a_i (\ln T^*)^i$  eq. 2-23

$T^*$  is the reduced temperature defined by:  $T^* = \frac{T}{\epsilon/k_B}$  and  $\frac{\epsilon}{k_B}$  is the energy scaling parameter.

**Table 2: Coefficients used to calculate reduced effective collision cross section**

i	a <sub>i</sub>	
0	0.355404	$\epsilon/k_B = 299.363$
1	-0.464337	$\sigma = 0.468 \text{ nm}$
2	0.0257353	$M = 102.031 \text{ kg/kmol}$

$B_\eta(T)$  is the second viscosity virial coefficient calculated by:

$$B_\eta(T) = N_A \sigma^3 \sum_{i=0}^8 b_i (T^*)^{t_i} \text{eq. 2-24}$$

Where  $N_A$  is avogadro's number and the coefficients used are given by table 3.

**Table 3: Parameters used to solve for 2nd viscosity virial coefficient**

i	b <sub>i</sub>	t <sub>i</sub>	i	b <sub>i</sub>	t <sub>i</sub>
0	-19.572881	0	5	2491.6597	-1.25
1	219.73999	-0.25	6	-787.26086	-1.5
2	-1015.3226	-0.5	7	14.085455	-2.5
3	2471.0125	-0.75	8	-0.34664158	-5.5

4	-3375.1717	-1			
---	------------	----	--	--	--

Higher density terms contribution  $\Delta_H\eta(\rho, T)$  is calculated in mPa.s by:

$$\Delta_H\eta(\rho, T) = c_1\delta + \left( \frac{c_2}{\tau^{*6}} + \frac{c_3}{\tau^{*2}} + \frac{c_4}{\sqrt{\tau^*}} + c_5\tau^{*2} \right) \delta^2$$

$$+ c_6\delta^3 + \frac{c_7}{\delta_0(\tau^*) - \delta} - \frac{c_7}{\delta_0(\tau^*)} \text{eq. 2-25}$$

$$\text{Where: } \tau^* = \frac{T}{T_c}, \delta = \frac{\rho}{\rho_c}, \delta_0(\tau^*) = \frac{c_{10}}{1 + c_8\tau^* + c_9\tau^{*2}} \text{eq. 2-26}$$

**Table 4: Parameters used to calculate Higher density terms**

i	c <sub>i</sub>	i	c <sub>i</sub>
1	-0.0206900719	6	-0.00351593275
2	0.000356029549	7	0.214763320
3	0.00211101816	8	-0.0890173375
4	0.0139601415	9	0.100035295
5	-0.00456435020	10	3.163695636

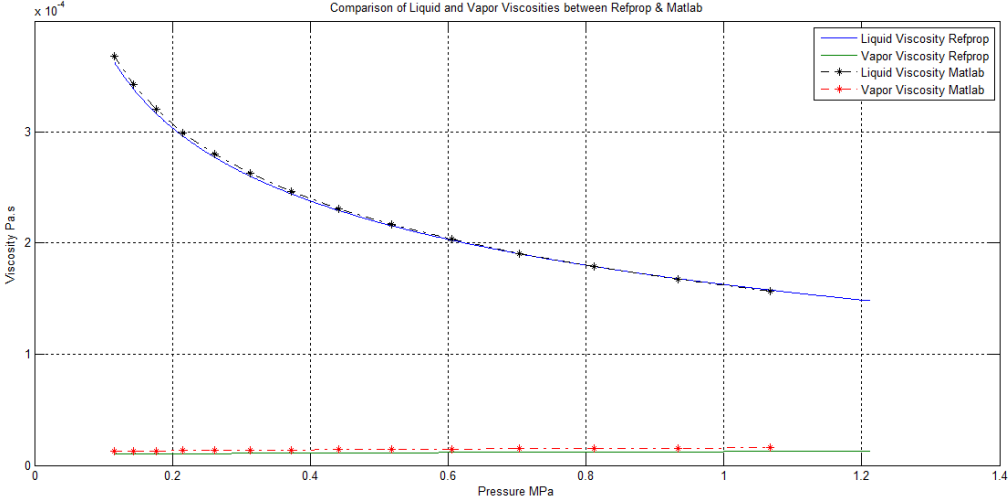


**Figure 4: Comparison of Liquid and Vapor viscosities generated by Refprop and Matlab**

Figure 4 shows good agreement between Refprop and our Matlab code in regards to liquid and vapor viscosities w.r.t. pressure.

### C. Thermal Conductivity of R134a

McLinden et al[32] formulated the following expression for R134a thermal conductivity:

$$\lambda(T, \rho) = \lambda^{int}(T) + \lambda^*(T) + \lambda^r(T, \rho) + \lambda^{crit}(T, \rho) \text{eq. 2-27}$$

Where  $\lambda^{int}(T)$  is thermal conductivity due to contribution from internal motions of the molecule,  $\lambda^*(T)$  is the ideal gas contribution,  $\lambda^r(T, \rho)$  is the residual part contribution, and  $\lambda^{crit}(T, \rho)$  is the critical part.

$$\lambda^{int}(T) \text{ is given by: } \lambda^{int}(T) = \frac{f_{int} \eta^*(T)}{M} [C_P^* - 2.5 R_{molar}] \text{W/m.Keq. 2-28}$$

where  $C_P^*$  (J/mol.k ) is the ideal-gas heat capacity,  $R_{molar}$ (J/mol.k ) is the gas constant,  $M$ (kg/kmol) is the molar mass, and  $\eta^*(T)$  is the ideal gas viscosity.

Using R. Tillner-Roth and H. Baehr [26]:

$$C_p^* = R \left( -0.629789 + \frac{7.292937}{\sqrt{\tau}} + \frac{5.154411}{\sqrt[4]{\tau^3}} \right) \text{eq. 2-29}$$

$$\lambda^*(T) = \frac{15 R_{molar} \eta^*(T)}{4M} \text{where unit of } \lambda^*(T) \text{ is mW/mkeq. 2-30}$$

$$\lambda^r(T, \rho) = b_1 \delta + b_2 \delta^2 + b_3 \delta^3 + b_4 \delta^4 \text{eq. 2-31}$$

Where  $b_1 = 0.00377406$ ,  $b_2 = 0.0105342$ ,  $b_3 = -0.00295279$ ,  $b_4 = 0.00128672592$

$$\lambda^{crit}(T, \rho) = \rho C_p \frac{R_0 K T}{6\pi \eta \xi} (\Omega - \Omega_0) \text{eq. 2-32}$$

Where  $\eta$  is the dynamic viscosity,  $C_p$  is the isobaric heat capacity,  $K$  is boltzman constant,  $R_0$  is a universal amplitude of the value 0.69,

$$\xi \text{ is the correlation length given by: } \xi = \xi_0 \left[ \frac{1}{\Gamma} (\chi^*(T, \rho) - \chi^*(T_{ref}, \rho)) \right]^{0.50487} \text{eq. 2-33}$$

$$\chi^*(T, \rho) \text{ is the dimensionless susceptibility: } \chi^*(T, \rho) = \frac{\rho P^{crit}}{(\rho^{crit})^2} \left( \frac{\partial \rho}{\partial P} \right)_T \text{eq. 2-34}$$

$$\Gamma = 0.0496, \text{ Assume } T_{ref} = 1.5T$$

$$\left( \frac{\partial \rho}{\partial P} \right)_T = \frac{1}{RT(1+2\delta\Phi_{\delta\delta}^r + \delta^2\Phi_{\delta\delta}^r)} \text{eq. 2-35}$$

The crossover functions  $\Omega$  and  $\Omega_0$  are given by:

$$\Omega = \frac{2}{\pi} \left[ \left( \frac{C_p - C_v}{C_p} \right) \tan^{-1}(q_D \xi) + \frac{C_v}{C_p} q_D \xi \right] \text{eq. 2-36}$$

$$\Omega_0 = \frac{2}{\pi} \left\{ 1 - \exp \left[ \frac{-1}{(q_D \xi)^{-1} + \frac{1}{3} \left( \frac{q_D \xi \rho^{crit}}{\rho} \right)^2} \right] \right\} \text{eq. 2-37}$$

The modified effective cutoff wave number  $q_D$  is  $1.89202 \times 10^9 \text{ m}^{-1}$ .

Figure 5 shows good agreement between liquid and vapor thermal conductivities predicted by Matlab and Refprop.

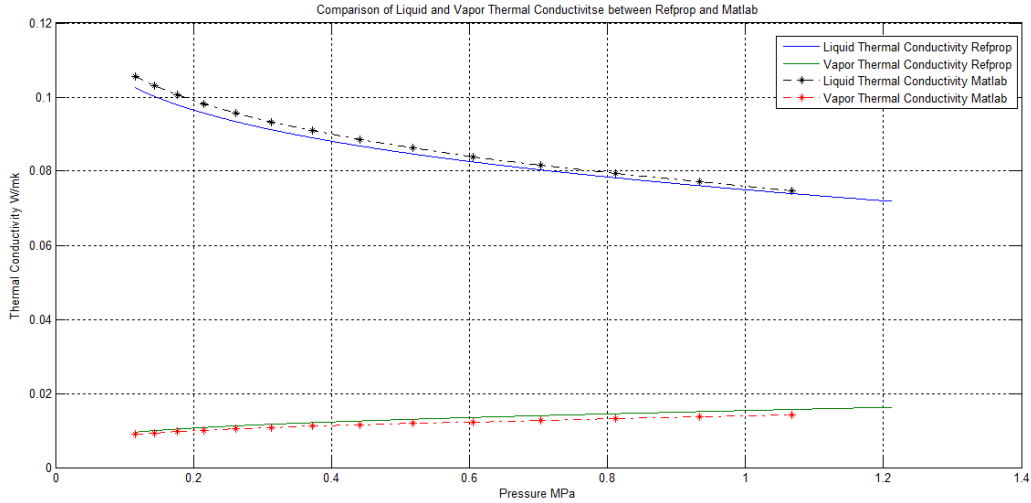


Figure 5: Comparison of Liquid and Thermal Conductivities between Refprop and Matlab

#### D.Surface Tension of R134a

A. Mulero et al [33] proposed a modification of the surface tension equation used in Refprop and proposed initially by Okada and Higashi[34]. The equation used to calculate the surface tension of R134a is the following:

$$\sigma(T) = \sigma_0 \left(1 - \frac{T}{T_c}\right)^n$$

Where  $\sigma_0 = 0.05801 \text{ N/m}$  and  $n = 1.241$

Figure 6 shows the comparison between surface tension generated by Matlab and that of Refprop.

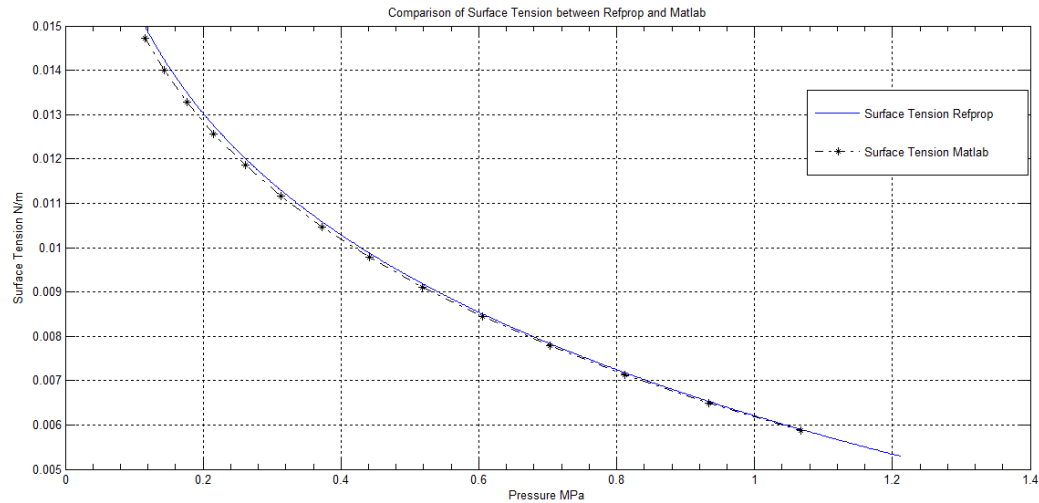


Figure 6: Comparison of Surface Tension between Refprop and Matlab

## CHAPTER III

### CONSTANT HEAT FLUX - NO AXIAL HEAT CONDUCTION

#### SOLUTION METHODOLOGY & RESULTS

##### A. Mathematical Model

Fayssal and Moukalled [3] studied steady two phase flow of refrigerants in evaporators and condensers under constant heat flux. [3] assumed one-dimensional annular flow through the pipe with steady state conditions. Same conditions will be used to check out the accuracy of our

mathematical model. A brief description of the problem and the governing equations will be mentioned since these equations will be the basis of other chapters.

Figure 7 shows a cross section of a pipe resembling the heat exchanger coil in evaporation and condensation cases. At each control volume CV, inlet conditions as saturation pressure, liquid density, vapor density, liquid enthalpy, vapor enthalpy, and flow quality are known either as boundary conditions for the 1<sup>st</sup> control volume or as outputs of the outlet face calculations of previous CV. Finite volume method will be used to solve for the conservation of continuity, energy, and momentum equations. These equations will be solved using MATLAB software.

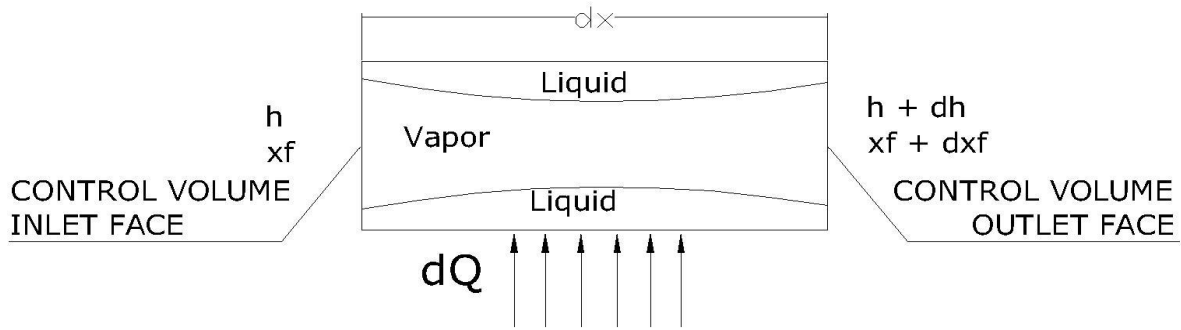


Figure 7: Cross section of heat exchanger pipe

### 1. Continuity Equation

$$\nabla \cdot (\alpha_v \rho_v \vec{V}_v) + \nabla \cdot (\alpha_l \rho_l \vec{V}_l) = 0 \text{ eq. 3-1}$$

Where the vapor continuity equation during evaporation is:  $\nabla \cdot (\alpha_v \rho_v \vec{V}_v) = \dot{M}$  eq. 3-1a

And the liquid continuity equation during evaporation is:  $\nabla \cdot (\alpha_l \rho_l \vec{V}_l) = -\dot{M}$  eq. 3-1b

$\dot{M}$  is the mass rate of vapor refrigerant formed, that is the mass rate of liquid refrigerant disappearing,  $\alpha_v$  and  $\alpha_l$  the vapor and liquid volume fractions respectively where  $\alpha_v + \alpha_l = 0$

Notice that  $\dot{M}$  depends on the wall heat flux applied via the following relation:

$$\dot{M} = \frac{4\sqrt{\alpha_v}\ddot{Q}_w}{D_i i_{fg}} \text{(Sensible heat between liq. and vap. interfaces is negligible)eq. 3-1c}$$

## 2. Energy Equation

Several forms of energy equations can be used. Since our work focuses on two phase flow only, energy conservation of a control volume will be used to solve for the change in energy of refrigerant at control volume faces.

$$\dot{m} dh = dQ = dS \ddot{Q}_w = \pi D_i dx \ddot{Q}_w \text{eq. 3-2}$$

## 3. Momentum Equation

Both liquid and vapor phases share the same pressure field. The combined momentum equation used to solve for pressure at any outlet face is of the following form:

$$\nabla(\alpha_v \rho_v V_v^2) + \nabla(\alpha_l \rho_l V_l^2) = -\nabla P + \frac{4}{D_i} \tau \quad \text{eq. 3-3}$$

(Gravitational forces are neglected since pipe is assumed horizontal)

### a. Wall Shear Stress Calculation

$\tau$  is the wall shear stress. It is calculated using the following expression:

$$\tau = -f_{lo} \phi_{lo}^2 \frac{G_R^2}{2\rho_l} = -f_{lo} \frac{G_R^2}{2\rho_l} \left( E + \frac{3.24LH}{Fr^{0.045} We^{0.035}} \right) \text{eq. 3-4}$$

$$\text{Where } E = (1 - x_f)^2 + x_f^2 \frac{\rho_l f_{vo}}{\rho_v f_{lo}}, L = x_f^{0.78} (1 - x_f)^{0.224} \text{eq. 3-4a,b}$$

$$H = \left( \frac{\rho_l}{\rho_v} \right)^{0.91} \left( \frac{\mu_v}{\mu_l} \right)^{0.19} \left( 1 - \frac{\mu_v}{\mu_l} \right)^{0.7}, We = \frac{G_R^2 D_i}{\rho_h \sigma}, Fr = \frac{G_R^2}{g D_i \rho_h^2} \text{eq. 3-4c,d,e}$$

$$\rho_h = \frac{\rho_l \rho_v}{\rho_l x_f + (1 - x_f) \rho_v} \text{eq. 3-4f}$$

Note that any friction factor is calculated using  $f = \frac{f_{DC}}{4}$  where:



$$\frac{1}{\sqrt{f_{DC}}} = -1.8 \log \left[ \frac{6.8}{Re} + \left( \frac{\varepsilon/D_i}{3.7} \right)^{1.11} \right] \text{eq. 3-4g}$$

Calculating  $Re_l$  means using liquid velocity in the calculation, whereas using the vapor velocity ends with  $Re_v$ . To find  $f_{lo}$  and  $f_{vo}$  used in eq. 3-4a, total mass flux must be used in calculating Reynolds number thus:

$$Re = \frac{G_R(1-x_f)D_i}{\mu} \text{eq. 3-4h}$$

For more elaboration on the wall shear stress calculations revise [3] and [20].

## **B. Equations Discretization**

All equations will be discretized using finite volume method.

### ***1. Continuity Equation***

#### **a. Vapor Continuity Equation**

Integrate along the control volume of length dx

$$\int_V \nabla(\alpha_v \rho_v \vec{V}_v) dV = \int_V \dot{M} dV \text{eq. 3-5}$$

Use Gauss method to change the volume integral on the left hand side to surface integral. Evaluate  $\dot{M}$  at the control volume faces by taking it as the average of its value at the inlet and outlet control volume faces.

$$\oint_{\partial V} (\alpha_v \rho_v \vec{V}_v) \cdot \vec{dS} = \frac{\dot{M}_z + \dot{M}_{z+1}}{2} \int_V dV \text{eq. 3-5a}$$

Eq 3-5a becomes:

$[(\alpha_v \rho_v V_v)_{z+1} - (\alpha_v \rho_v V_v)_z] \frac{\pi D_i^2}{4} = \frac{\dot{M}_z + \dot{M}_{z+1}}{2} \frac{\pi D_i^2}{4} dx$  eq. 3-5b which can be simplified to:

$$\frac{[(\alpha_v \rho_v V_v)_{z+1} - (\alpha_v \rho_v V_v)_z]}{dx} = \frac{\dot{M}_z + \dot{M}_{z+1}}{2} \text{eq. 3-5c}$$

### b. Liquid Continuity Equation

$$\frac{(\alpha_l \rho_l V_l)_{z+1} - (\alpha_l \rho_l V_l)_z}{dx} = -\frac{\dot{M}_z + \dot{M}_{z+1}}{2} \text{eq. 3-6}$$

## **2. Energy Equation**

Integrate along the cylinder volume:

$$\int_V \dot{m} \frac{dh}{dx} = \int_V \pi D_i \ddot{Q}_w \text{eq. 3-7}$$

The energy equation becomes:

$$\dot{m} \Delta h S_f = \pi D_i \ddot{Q}_w \text{Volume}_{cylinder} \text{eq. 3-7a}$$

$$\dot{m} \Delta h = \dot{m} (h_{z+1} - h_z) = \pi D_i \ddot{Q}_w dx \text{eq. 3-7b}$$

Note that  $h_{z+1} = [i_l(1 - x_f) + i_v x_f]_{z+1}$  and  $h_z = [i_l(1 - x_f) + i_v x_f]_z$  are the inlet and outlet enthalpies of the control volume defined at the faces.

After changing the mass flow rate into mass flux the energy equation becomes:

$$[i_l(1 - x_f) + i_v x_f]_{z+1} - [i_l(1 - x_f) + i_v x_f]_z = \frac{4 \ddot{Q}_w dz}{G_R D_i} \text{eq. 3-7c}$$

Where:  $i_l$ ,  $i_v$ , and  $x_f$ , are liquid and vapor enthalpies, and flow quality respectively.

### a. Wall Temperature

Note that the wall temperature could be found from heat flux  $\ddot{Q}_w$  definition:

$$\ddot{Q}_w = h_{ref}(T_{w,int} - T_{refrigerant}) \quad \text{eq. 3-8}$$

Where  $h_{ref}$  is the heat transfer coefficient. Since the flow is annular (liquid film near the pipe wall and vapor in the center of the pipe):

$$h_{ref} = h_l \text{.where } h_l \text{ is the liquid heat transfer coefficient.}$$

$$h_l = 1.85 h_{fc} (Bo \cdot 10^4 + 1.5X^{\frac{2}{3}})^{0.6} \text{eq. 3-9}$$

$$\text{Where } h_{fc} = 0.023 \frac{k_l}{D_i} Re_l^{0.8} Pr_l^{0.4}, Bo = \frac{\ddot{Q}_w}{Gr_l fg}, \text{ and } X = \left(\frac{1-x_f}{x_f}\right)^{0.9} \left(\frac{\rho_v}{\rho_l}\right)^{0.5} \left(\frac{\mu_l}{\mu_v}\right)^{0.1}$$

$Bo$  is the boiling number, and  $X$  is Lockhart-Martinelli parameter

### 3.Momentum Equation

Using the control volume method, the combined momentum equation becomes:

$$\frac{(\alpha_v \rho_v V^2)_z + 1 - (\alpha_v \rho_v V^2)_z}{dz} + \frac{(\alpha_l \rho_l V^2)_z + 1 - (\alpha_l \rho_l V^2)_z}{dz} = -\frac{(P_{z+1} - P_z)}{dz} + \frac{4}{D_i} \left(\frac{\tau_z + \tau_{z+1}}{2}\right) \text{eq.3-10}$$

### C. Solution Algorithm

As mentioned, this study will predict hydrodynamic and thermal behavior during evaporation and condensation under constant or variable heat flux. This model can be used to determine proper size of heat exchangers to achieve full evaporation or condensation.

A pipe made up of one CV of length  $dx = 1mm$  will be taken into consideration as the evaporator initial pipe length guess. Calculations will proceed in each control volume to find the refrigerant's thermodynamic properties in addition to flow quality at the CV outlet face. In the evaporation process, a flow quality of 1 indicates that the liquid is totally transformed into vapor (in condensation, a flow quality of 0 indicates that the vapor is totally transformed into liquid).

Iterations will stop when flow quality of the studied control volume is 1 (0 in condensation). Number of control volumes will then be known thus the coil's optimal length will be calculated.

Note that the above equations are used if a constant heat flux or a variable one is applied. The algorithm to solve the problem is the same. The only difference is in the way  $\ddot{Q}_w$  is used. If  $\ddot{Q}_w$  is constant then it is used straightforward, while if we are dealing with variable heat flux or constant heat flux applied at the outer surface of the evaporator pipe with axial heat conduction through the pipe taken into consideration, then  $\ddot{Q}_w$  will be guessed and used. More elaboration on this procedure is mentioned later on.

The solution starts by guessing pressure at the control volume outlet face. From this value, using Helmholtz equations mentioned in chapter 2, find all needed thermodynamic properties (liquid and vapor enthalpies, temperature, liquid and vapor thermal conductivities, liquid and vapor densities, liquid and vapor viscosities, surface tension....).

Using *eq 3-7c*, find the flow quality at the outlet face. Use it to calculate void fraction  $\alpha_v$ .

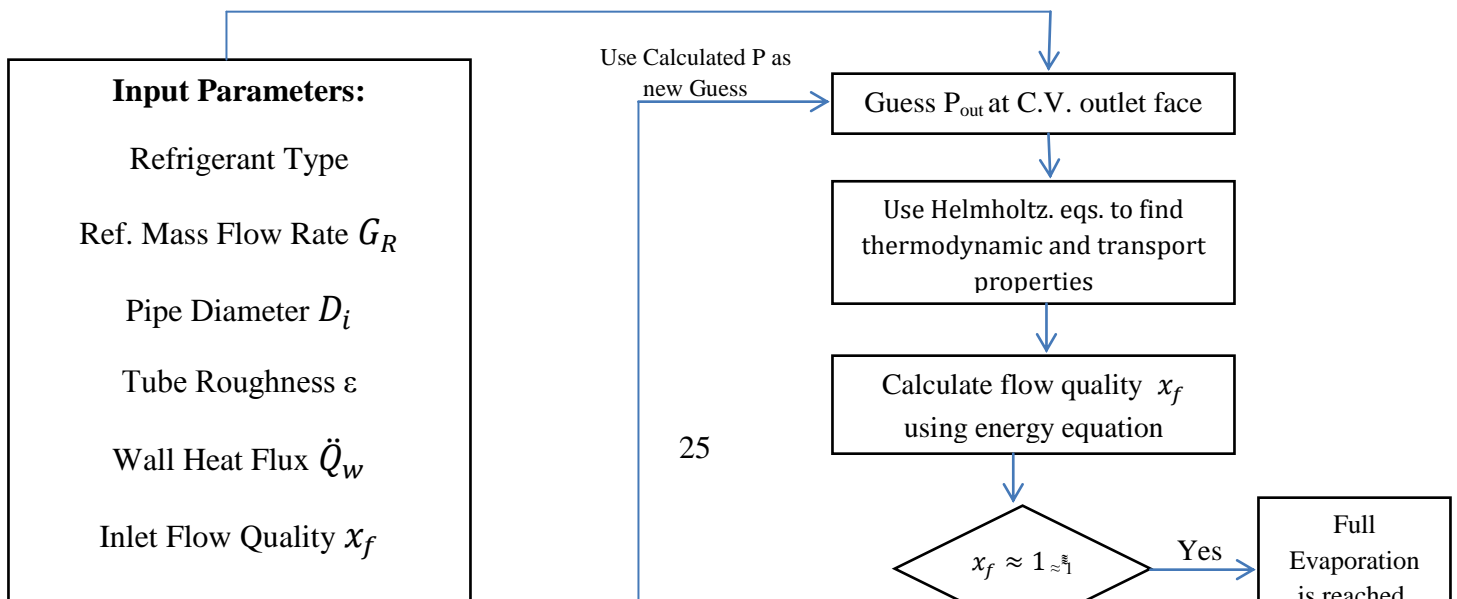
$$\alpha_v = \frac{1}{1 + \left(\frac{1-x_f}{x_f}\right) \left(\frac{\rho_v}{\rho_l}\right)^{\frac{2}{3}}} \text{eq. 3-11}$$

Determine liquid and vapor velocities using the continuity equations *eq.3-5c* and *eq.3-6*. Then update pressure at the outlet face using the momentum equation in *eq.3-8*. Check difference between calculated and guessed pressure. If value less than 0.0001, store all properties as the inlet conditions of the adjacent control volume which will be created. Continue with the

following procedure until flow quality approaches 1 in case of evaporation or 0 in case of condensation.

If pressure difference is not small enough, use the calculated pressure as the new guessed pressure at the control volume outlet and perform all steps mentioned above.

### C. Solution Flow Chart



## **D. Results**

Same conditions used in [3] will be used to validate our model, R12 will be used in the validation and then R134a will be the base refrigerant in our study:

### **R12 Evaporation process inputs:**

$$D_i = 1 \text{ cm}, \quad \varepsilon = 1.5 \times 10^{-6}, \quad P_0 = 0.37 \text{ Mpa}, x_f = 0.2, \ddot{Q}_w = 10000 \text{ W/m}^2,$$

$$\dot{m} = 0.0314 \text{ Kg/s}$$

Figure 8 shows the evaporation results of R12 subjected to constant heat flux. As expected there is an obvious pressure drop from 0.37 MPa to 0.3371 MPa at the last CV. The pressure drop is around 8.5% while that in [3] is around 6.8%.

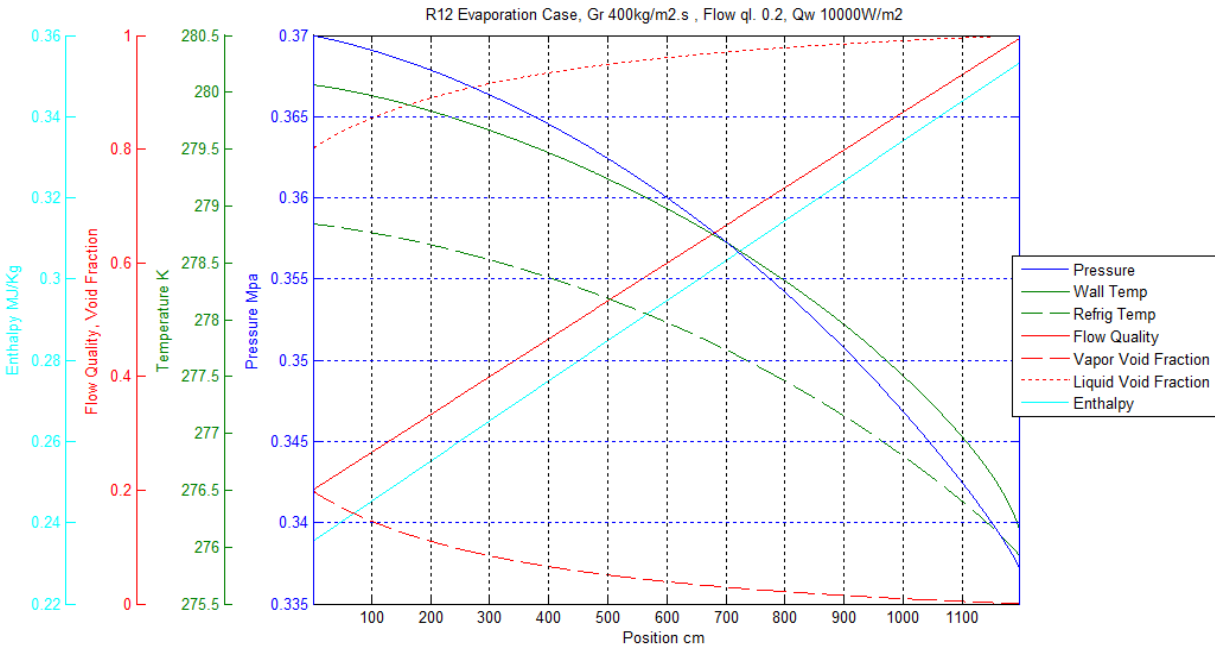


**Figure 8: Variation of pressure, refrigerant and heat exchanger wall temperature, enthalpy, flow quality, volume fraction of R12 during evaporation subjected to Constant Heat Flux**

According to M. Awad[35], Pressure drop is affected by frictional and acceleration forces (gravitational pressure drops aren't taken into consideration since the flow is horizontal).

The frictional pressure drop results from the shear stress between the fluid and the pipe wall and also from the shear stress between the liquid and gas phases. In our work we neglected the shear stress between the liquid and gas phases thus the frictional pressure drop contribution is solely related to the shear stress mentioned in *eq.3-4* which depends on the void fraction.

The acceleration component of pressure drop depends on the change in kinetic energy of the flow thus the liquid and vapor velocities.

Figures 8 and 9 show that the vapor volume fraction and vapor velocity are increasing from 0.8 to 1 and 4.5m/s to 18.6m/s respectively while the liquid volume fraction and liquid velocity are decreasing from 0.2 to 0 and 1.2 to 0.6 m/s (at 99.5% flow quality) respectively which can clearly explain the predicted pressure drop.

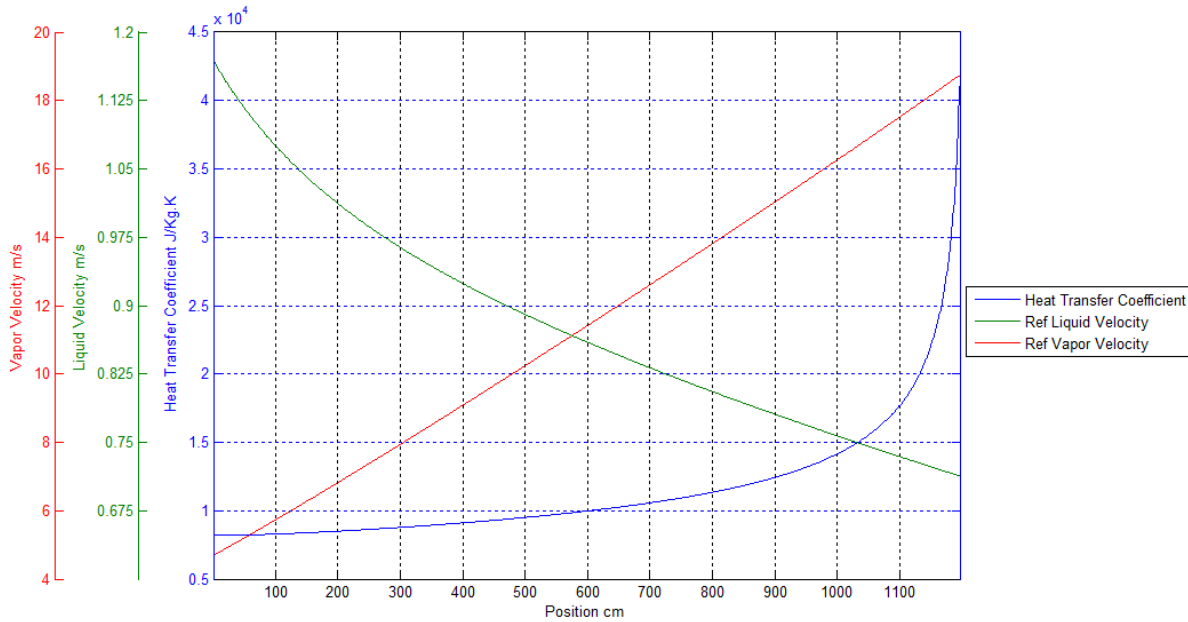


**Figure 9: Variation of heat transfer coefficient, liquid velocity, and vapor velocity of R12 during evaporation**

Wall and Refrigerant temperatures show great agreement with [3]. Both are decreasing which is expected since refrigerant temperature is correlated with saturation pressure, while pipe wall temperature is decreasing because, during an annular flow, the liquid film near the pipe wall is gradually decreasing thus its thermal resistance is decreasing which means more heat is transferred and this can be assured by noticing in Figure 8 the increase in heat transfer coefficient as flow marches with length.

Figure 9 shows a linear increase of the flow quality as in [3]. From the enthalpy and length variation we conclude that the evaporator dimensions are 11.98m in length and 1cm in diameter and its capacity is:



$$\dot{m} (h_{1198} - h_1) = 0.0314 \times (3.53336 - 2.35353) \times 10^5 = 3.74 \text{ KW}$$

**R12 Condensation process inputs:**

$$D_i = 1 \text{ cm}, \quad \varepsilon = 1.5 \times 10^{-6}, \quad P_0 = 1.02 \text{ Mpa}, \quad x_f = 1, \quad \ddot{Q}_w = 10000 \text{ W/m}^2,$$

$$\dot{m} = 0.0314 \text{ Kg/s}$$

Figure 10 show that the pressure drop during condensation is 0.6% (from 1.02MPa to 1.01323MPa) which is considered negligible and won't be taken into consideration during condensers design. This is due to the fact mentioned earlier where the acceleration component of the pressure drop opposes the frictional one. The kinetic energy of the fluid is decreasing while the vapor condenses completely to liquid as shown in the same figure where liquid volume fraction almost reached 1 at the end of the condensation process.(liquid volume fraction becomes 0.96 when the flow quality reaches 0.005) and where both liquid and vapor velocities decrease as shown in Figure11.

Wall temperature decreases rapidly as shown in Figure 10 as the heat transfer coefficient decreases as shown in Figure 11 so to compensate this decrease since the outward applied heat flux is constant and it is the product of the heat transfer coefficient and the difference in refrigerant and pipe wall temperature. As long as the imposed outward heat flux is constant the flow quality decreases linearly.

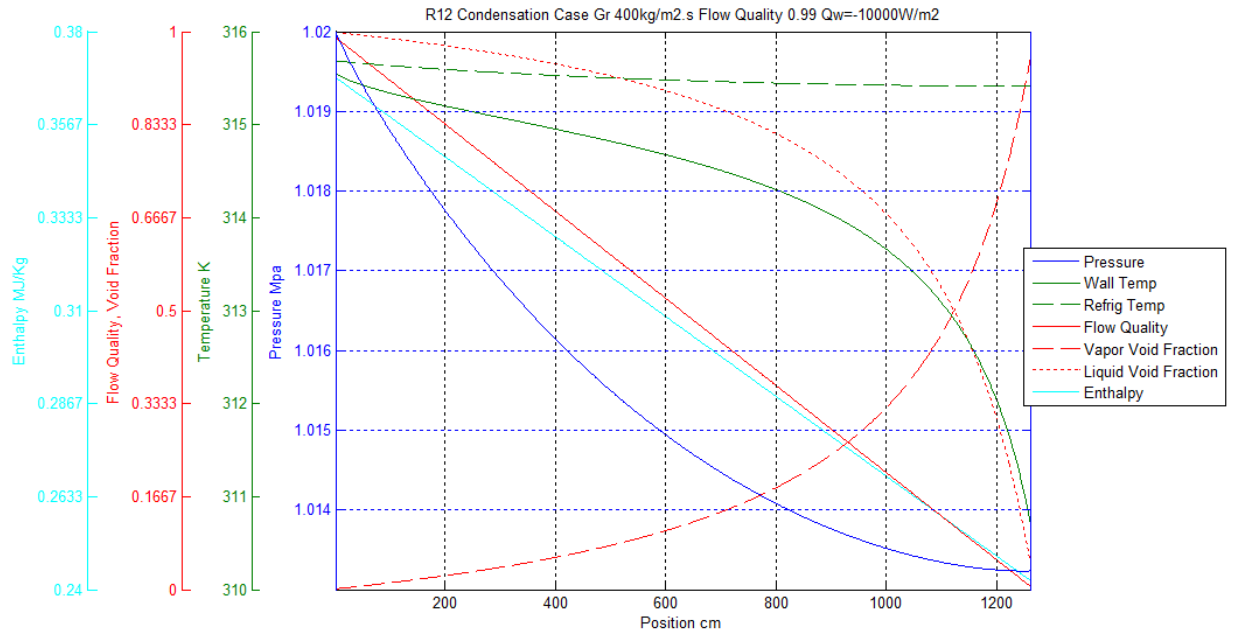


Figure 10: Variation of pressure, refrigerant and heat exchanger wall temperature, enthalpy, flow quality, volume fraction of R12 during condensation

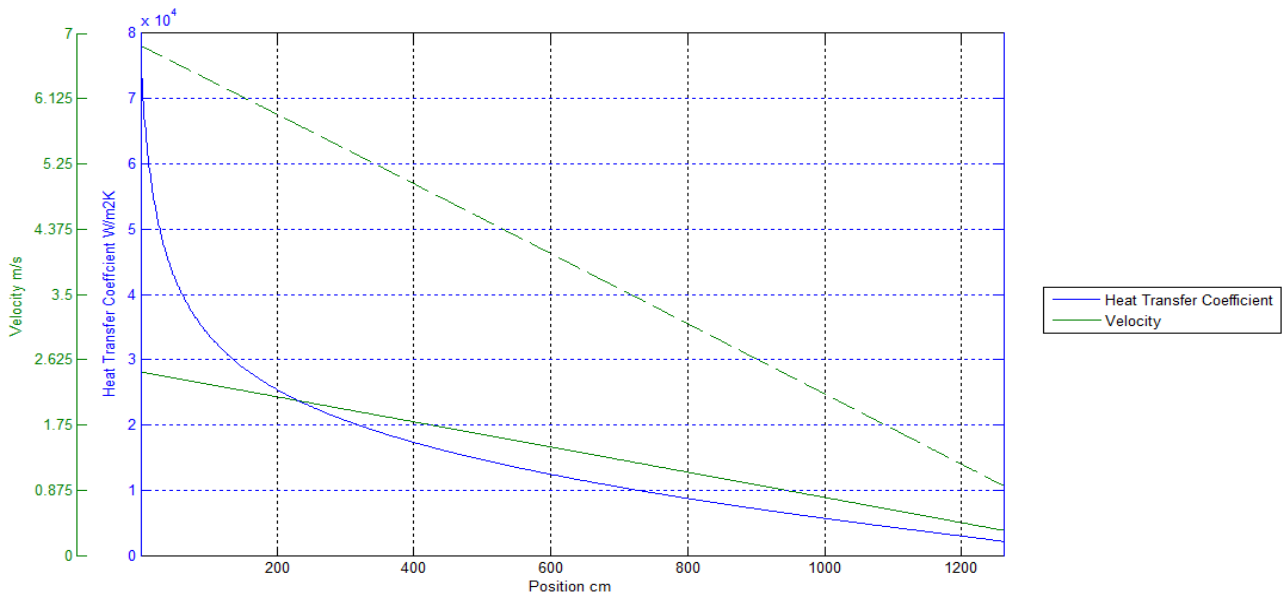


Figure 11: Variation of heat transfer coefficient, liquid velocity, and vapor velocity of R12 during condensation

Using the enthalpy change and the condenser length (12.63 m) the condenser capacity is

$$\text{determined to be: } \dot{m} (-h_{1263} + h_1) = 3.96 \text{ KW}$$

**R134a Evaporation process inputs:**

$$D_i = 1 \text{ cm}, D_o = 1.27 \text{ cm}, \varepsilon = 1.5 \times 10^{-6}, \quad P_0 = 0.37 \text{ Mpa}, \quad x_f = 0.2,$$

$$\ddot{Q}_w = 10000 \text{ W/m}^2, \quad \dot{m} = 0.0314 \text{ Kg/s}$$

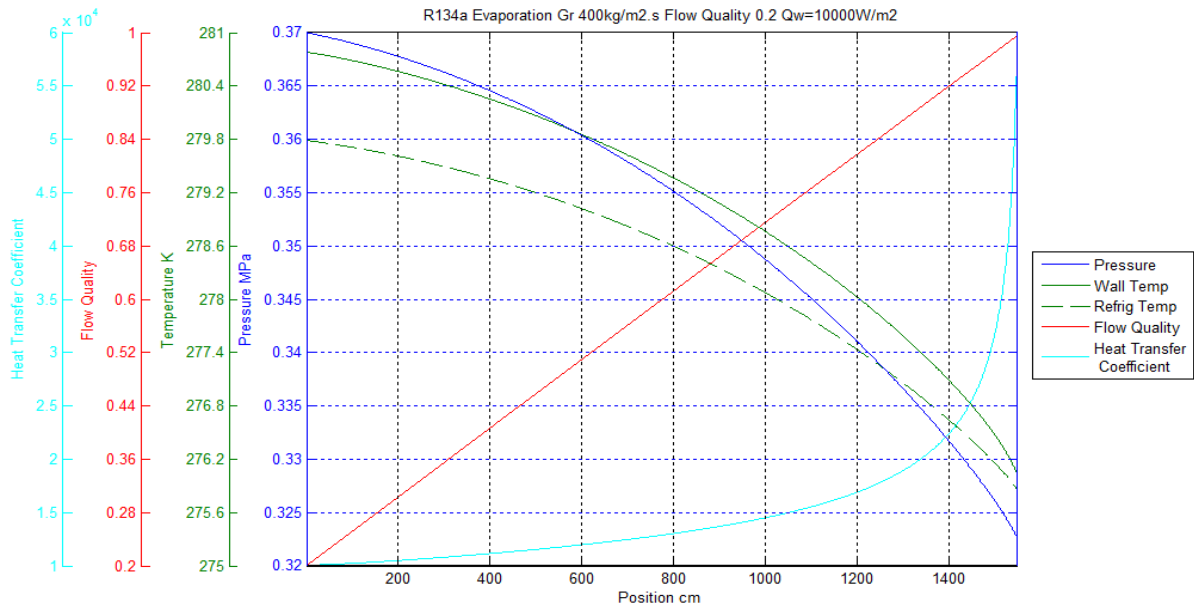


Figure 12: Variation of pressure, refrigerant and heat exchanger wall temperature, heat transfer coefficient, flow quality, of R134a during evaporation

Figure 12 shows that same patterns exist for flow quality variation, heat transfer coefficient, pressure... whether the refrigerant is R12 or R134a. The only difference is the length needed to reach full evaporation.

## CHAPTER IV

### VARIABLE HEAT FLUX - NO AXIAL HEAT CONDUCTION

#### SOLUTION METHODOLOGY & RESULTS

##### A. Mathematical Model

In this chapter, variable heat flux will be applied to the refrigerant wall and thus to the refrigerant. A double pipe heat exchanger will be used where the refrigerant passes in the inner tube and water in the outer tube. The inner pipe internal diameter will be denoted by  $D_i$  while the inner pipe outer diameter will be  $D_o$ . The outer pipe internal diameter will be denoted by  $D_s$ . See figures 13 and 14 below. Wall temperature discretization will be one dimensional and won't take into consideration radial variations since pipe thickness is very small.

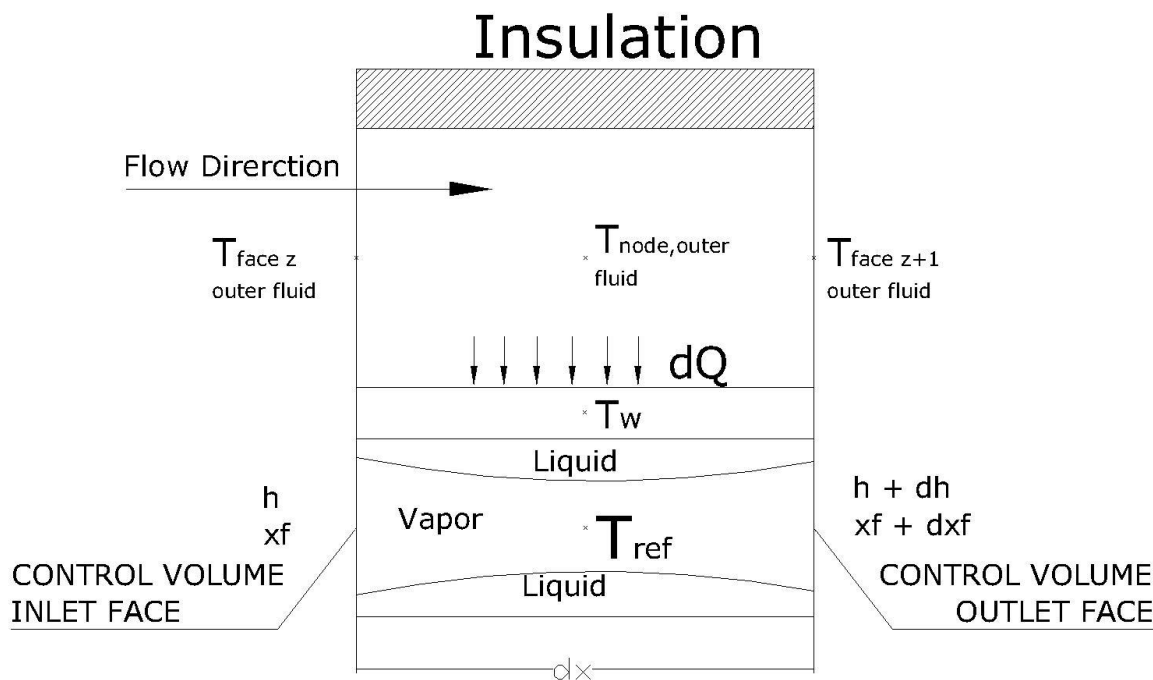


Figure 13: Cross section of concentric pipe

## Pipe & Annulus Diameters

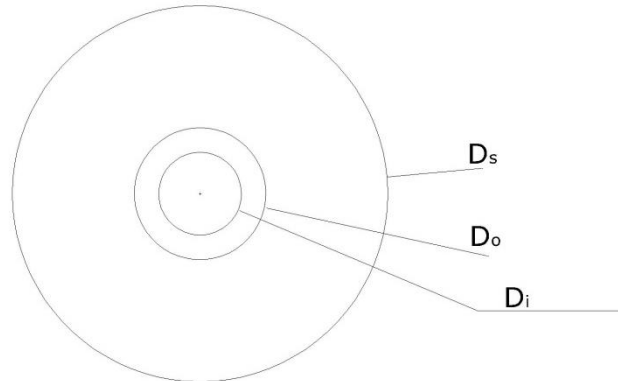


Figure 14: Dimensions of inner and outer pipe in concentric pipe

The outer fluid flow will be either parallel to the refrigerant or in the counter direction. Mass flow rate and inlet temperature of outer fluid will be specified. Governing equations used in chapter 3 for dealing with constant heat flux apply in this chapter also. The only difference is in the inner pipe heat flux value  $\ddot{Q}_w$ .

Note that:

$$\ddot{Q}_w = \frac{Q_w}{A_i} = \frac{Q_w}{\pi D_i dx} = h_{ref}(T_{wall,node z} - T_{ref,node z}) \text{eq. 4-1}$$

Where both wall and refrigerant temperatures are defined at control volume centers.

To solve for heat flux, two additional equations will be solved.

Heat transmitted to inner pipe = Heat transmitted from outer pipe

$$Q_w = \ddot{Q}_w \pi D_i dx = \ddot{Q}_{outer fluid} \pi D_o dx = h_{out fluid} \pi D_o dx (T_{wall,node z} - T_{of,node z}) \text{eq. 4-2}$$

Heat gained by refrigerant = Heat lost by outer fluid

$$Q_w = \dot{m}_{out fluid} C_{p_{out fluid}} (T_{out fluid_z} - T_{out fluid_{z+1}}) \text{eq. 4-3}$$

Where  $T_{outer\ fluid_z}$  and  $T_{outer\ fluid_{z+1}}$  are both defined at the control volume faces.

Wall heat flux  $\dot{Q}_w$  is applied at the circumference of the control volume. It depends on the difference of temperature between control volume centers. All other properties are defined on the faces. Note that with some modification on eq. 4-1 and eq. 4-2, a relation between outer fluid temperature and refrigerant temperature is obtained.

$$Q_w = \frac{T_{outer\ fluid} - T_{refrigerant}}{R_{total}} \text{eq. 4-4}$$

Where  $R_{total}$  is the refrigerant-pipe-outer fluid thermal resistance defined by:

$$R_{total} = R_{ref} + R_{pipe} + R_{outer\ fluid} \text{eq. 4-5}$$

$$R_{ref} = \frac{1}{\pi D_i dx h_i} \text{eq. 4-5a}$$

$$R_{cyl} = \frac{\log\left(\frac{D_o}{D_i}\right)}{2 \pi dx k_{pipe}} \text{eq. 4-5b}$$

$$R_{out\ fluid} = \frac{1}{\pi D_o dx h_{out\ fluid}} \text{eq. 4-5c}$$

## B. Solution Method for Parallel Flow

Same procedure used in chapter 3 will be used to solve for full evaporation. Outlet pressure is to be guessed, thus all thermodynamic properties of refrigerant are determined at face  $z+1$ . Also outer fluid temperature at control volume outlet face is guessed.

Average of inlet and outlet face temperatures of both the refrigerant and the outer fluid will be used as control volume node temperatures. Then inner pipe wall heat flux  $\ddot{Q}_w$  is calculated using eq. 4-1 and eq. 4-4.

Flow quality is found using eq. 3-7c and all equations mentioned in Chapter 3 are solved.

Outer fluid temperature is updated using eq. 4-3. If the difference between outer fluid temperature calculated and outer fluid temperature guessed is minimal, increment length by  $dx$  and create new control volume.

### C. Solution Method for Counter Flow

Some discrepancies are present when solving for counter flow evaporation. Pipe length is unknown and thus no info is available for the pressure of refrigerant at the last control volume. Outer fluid inlet temperature must be specified at the end of the pipe. This is the only information known about the outer fluid temperature.

The procedure to solve for full evaporation in the counter flow heat exchanger case is the following. Guess outer fluid temperature at the beginning of the pipe. Perform all steps mentioned for parallel flow but instead of using eq. 4-3 use the following equation.

$$Q_w = \dot{m}_{out\ fluid} C_{p_{out\ fluid}} (T_{outer\ fluid_{z+1}} - T_{outer\ fluid_z}) \text{eq. 4-6}$$

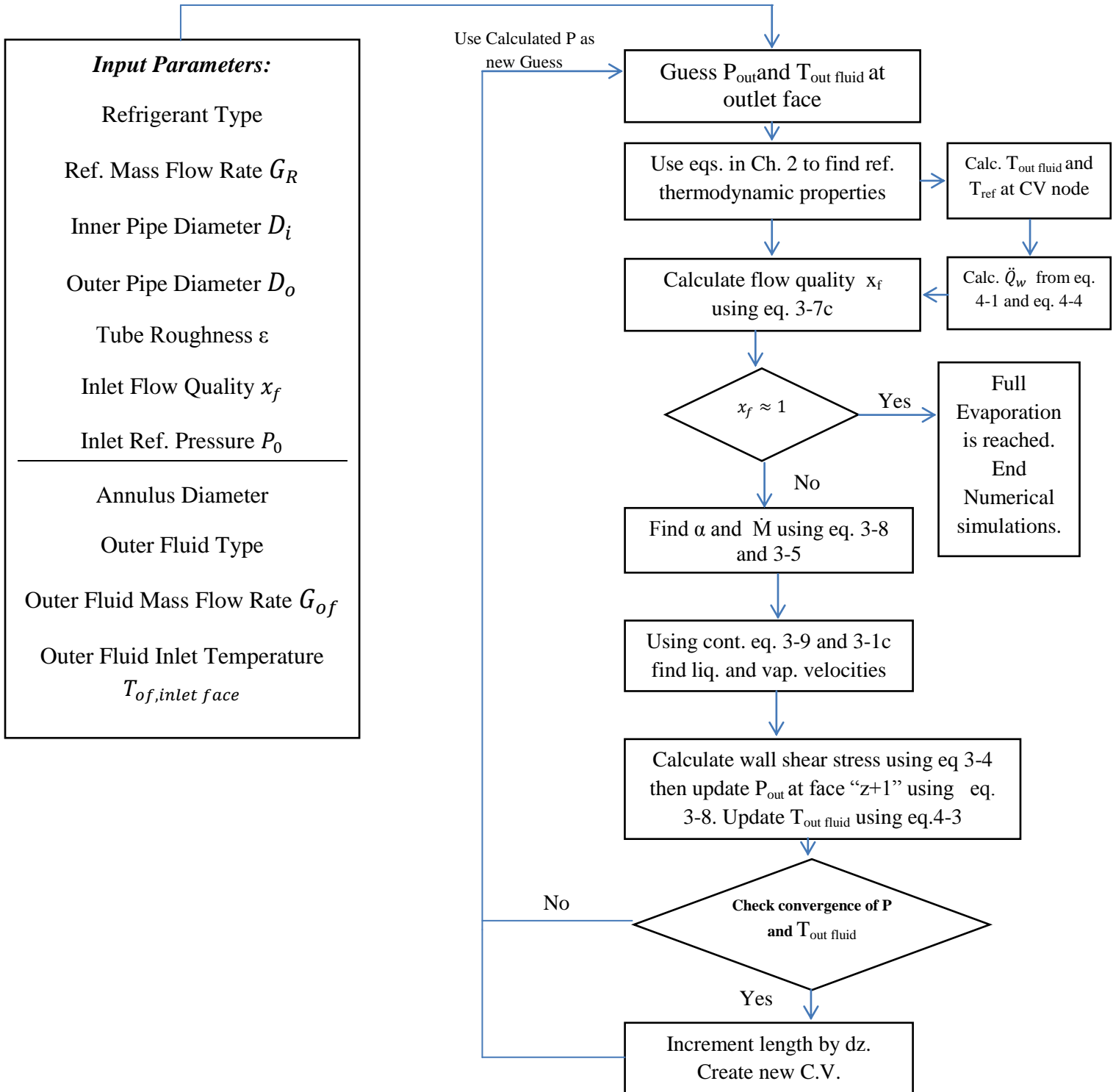
Which clearly means that the outer fluid temperature is increasing as evaporation occurs. After reaching full evaporation check outer fluid temperature at the last control volume and compare it with the specified or given outer fluid temperature. If the difference is less than  $0.005^\circ\text{C}$  stop the simulations. If not, a new outer fluid guess must be chosen in a way to speed the convergence process.

In this work, the following way to reach convergence was used:

- a) If outer fluid temperature calculated at the last control volume is less than the given outer fluid temperature, multiply the difference between the calculated outer fluid temperature at the last control volume and the given outer fluid temperature by a certain factor between 0 & 1 (we chose 0.5) and add the value to the old guess. Thus we have a new guess. Try it till convergence is reached.
- b) If outer fluid temperature calculated at the last control volume is greater than the given outer fluid temperature, multiply the difference between the calculated outer fluid temperature at the last control volume and the given outer fluid temperature by a certain factor between 0 & 1 (we chose 0.3) and subtract the value from the old guess. Thus we have a new guess. Try it till convergence is reached.



### D. Solution Flow Chart for Parallel Flow



## E. Results

As mentioned in chapter 3, the base case used from now on will depend on R134a as the refrigerant under study. In order to validate our mathematical model, and due to the lack of full detailed numerical simulations in the literature, the following approach was used. Outer fluid input parameters will be chosen in a way to have the average of imposed heat flux on the refrigerant has the value of 10000 W/m<sup>2</sup>.

Same input conditions used in chapter 3 for the refrigerant will be used that is:

### R134a Evaporation process inputs with parallel flow of outer fluid:

$$D_i = 1 \text{ cm}, D_o = 1.27 \text{ cm} \varepsilon = 1.5 \times 10^{-6} , \quad P_0 = 0.37 \text{ Mpa} , \quad x_f = 0.2$$

$$\dot{m}_{ref} = 0.0314 \text{ Kg/s} \text{ or } G_w = 400 \text{ Kg/m}^2\text{s}$$

Outer fluid needed inputs are: Annulus Diameter:  $D_s = 2.8 \text{ cm}$ , Outer Fluid Type: Water, Water

Mass Flow Rate  $G_w = 114 \text{ Kg/m}^2\text{s}$ , Water Inlet Temp.  $T_{w,inlet \text{ face}} = 300\text{K}$

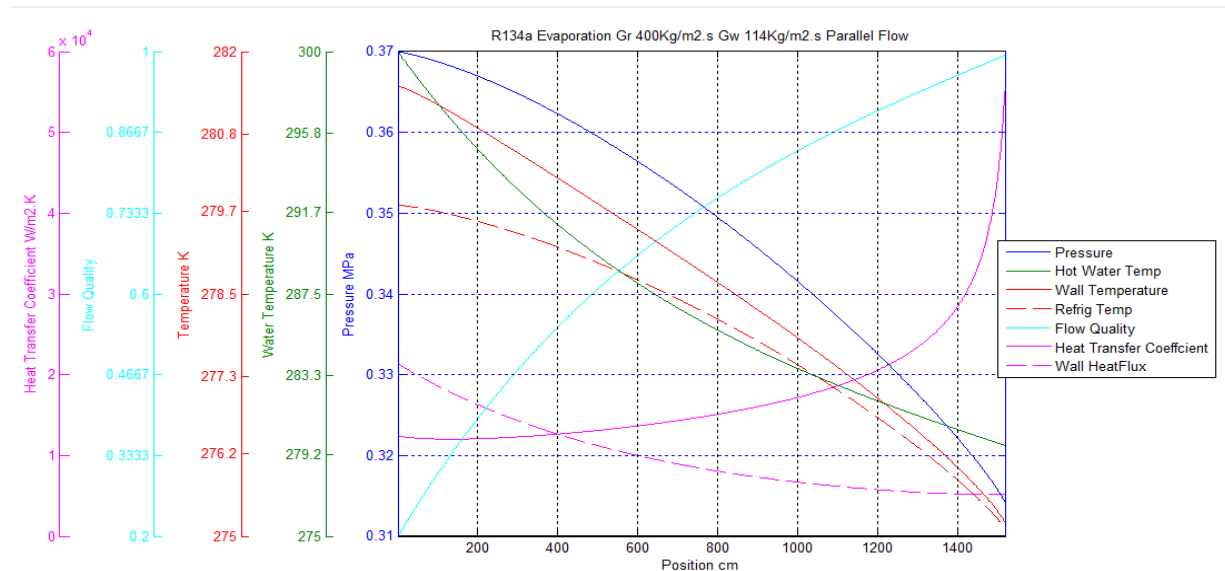
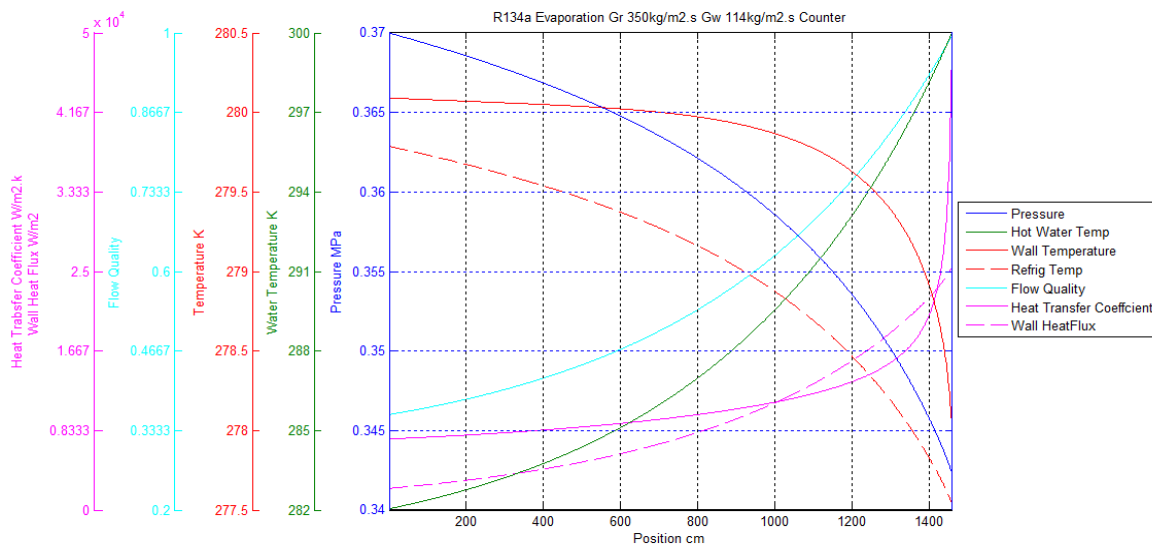


Figure 15: Variation of pressure, refrigerant and heat exchanger wall temperature, water temperature, heat transfer coefficient, and flow quality of R134a during evaporation subjected to variable heat flux, parallel

Results from both cases, the constant heat flux and the variable one, have the same trend. As shown in figure 15, the wall heat flux varies from  $2.1 \times 10^4 \text{ W/m}^2 \cdot \text{K}$  at pipe inlet to reach  $0.52 \times 10^4 \text{ W/m}^2 \cdot \text{K}$  at the pipe extremity. Its average is around  $10000 \text{ W/m}^2 \cdot \text{K}$ .

The length needed to reach full evaporation is  $15.21 \text{ m}$  while that in the constant case is  $15.48 \text{ m}$ . Flow quality variation isn't linear but follows a predicted pattern related to the wall heat flux where it increases rapidly when the heat flux is at its peak and then continues increasing to reach a flow quality of 1 but in a slower manner since the heat flux is decreasing. Wall and refrigerant temperature difference decreases from a max of  $2^\circ\text{C}$  to almost  $0^\circ\text{C}$  at the end of the evaporation process. Heat transfer coefficient increases as we approach full evaporation since as we mentioned earlier the thermal resistance of the refrigerant decreases as flow quality increases. The decrease in pressure drop in both cases is approximately the same. Hot water temperature decreases as the refrigerant is gaining its heat to reach  $279.4^\circ\text{C}$  with a total drop of  $20.6^\circ\text{C}$ .



**Figure 16: Variation of pressure, refrigerant and heat exchanger wall temperature, water temperature, heat transfer coefficient, and flow quality of R134a during evaporation subjected to variable heat flux, counter flow**

**R134a Evaporation process inputs with counter flow of outer fluid:**

$D_i = 1 \text{ cm}, D_o = 1.27 \text{ cm}, \varepsilon = 1.5 \times 10^{-6}, P_0 = 0.37 \text{ Mpa}, x_f = 0.2$ , Refrigerant

mass flux  $G_r = 350 \text{ Kg/m}^2\text{s}, D_s = 2.8 \text{ cm},$  Outer Fluid Type: Water,

Water Mass Flow Rate  $G_w = 114 \text{ Kg/m}^2\text{s},$  Water Inlet Temp.  $T_{w,inlet \text{ face}} = 300\text{K}$

Figure 16 shows the correlation between wall heat flux and flow quality as they change with the same pattern. The same applies for water temperature and refrigerant temperature as the difference between them decreases in the same rate as that of the flow quality. The heat transfer coefficient and the pipe wall temperature have their own pattern of changing compared to refrigerant and water temperature but follow the same trend compared to each other.

## CHAPTER V

### CONSTANT HEAT FLUX - AXIAL HEAT CONDUCTION

#### SOLUTION METHODOLOGY & RESULTS

##### A. Mathematical Model

In this chapter, constant heat flux will be applied to the inner pipe outer wall. The inner pipe internal diameter will be denoted by  $D_i$  while the inner pipe outer diameter will be  $D_o$ . See figure 17 below.

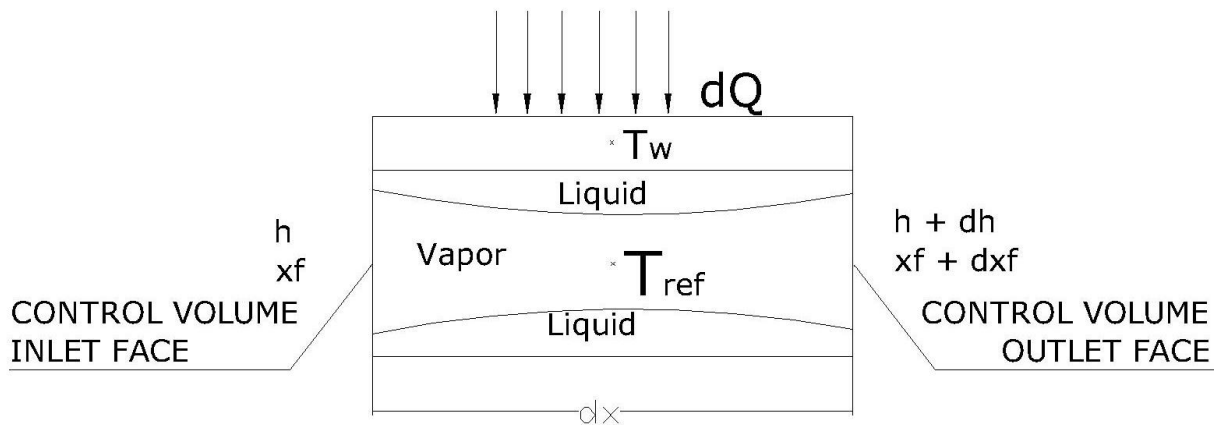


Figure 17: Cross section of evaporator pipe

If axial heat conduction is assumed to propagate in the pipe wall, heat flux propagating through the outer wall of the pipe  $\ddot{Q}_{w,out}$  is not totally transferred to the refrigerant. Some of the heat is passing to the surrounding control volumes of the pipe wall. Thus the heat transferred to the refrigerant is the heat input at the outer wall pipe minus the heat transferred to surrounding control volumes.

## B. Solution Method

Same procedure used in chapter 3 will be used to solve for full evaporation. Outlet pressure is to be guessed, thus all thermodynamic properties of refrigerant are determined at face  $z+1$ . Wall temperature field will be guessed thus wall temperature at node center and refrigerant temperature at node center are calculated and used to calculate inner pipe wall heat flux  $\ddot{Q}_w$ . Flow quality is found using eq. 3-7c and all equations mentioned in Chapter 3 are solved.

### 1. Pipe Wall Energy Equation

Energy equation of the pipe wall must be solved in order to find the accurate value of wall pipe temperature field. Simply, the sum of heat fluxes entering one control volume at the pipe wall must be zero. See figure 18.

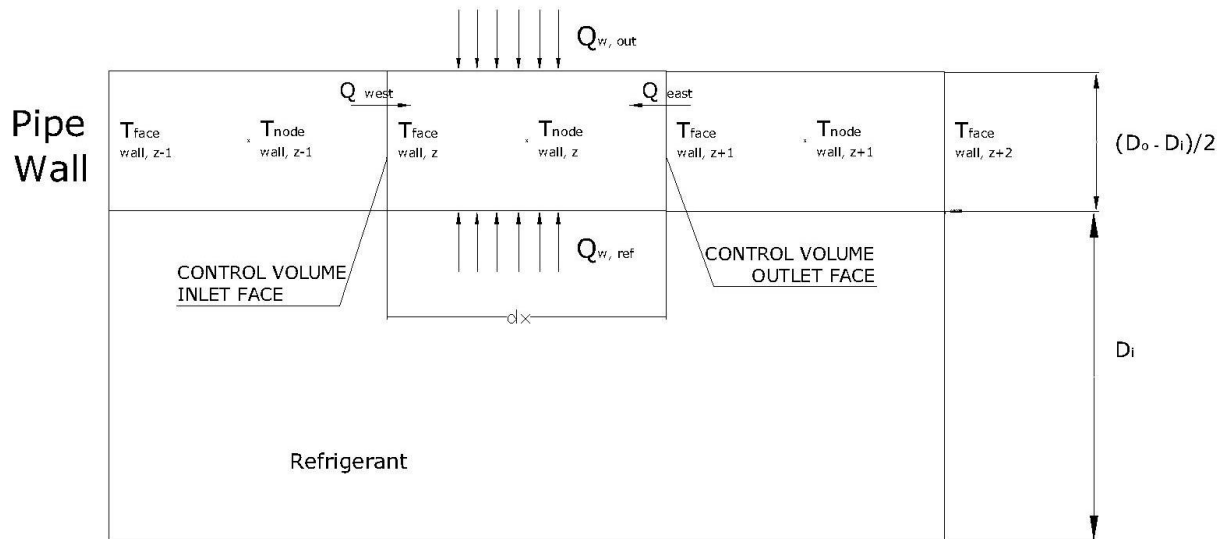


Figure 18: Section showing pipe wall grid

$$Q_{w,out} + Q_{w,in} + Q_{east} + Q_{west} = 0 \text{ eq. 5-1}$$

$$\begin{aligned} \ddot{Q}_{w,out} \pi D_o dx + \pi D_i dx h_l (T_{ref,node z} - T_{wall,node z}) + \frac{k_{pipe} A_{pipe}}{dx} (T_{wall,node z+1} - \\ T_{wall,node z}) + \frac{k_{pipe} A_{pipe}}{dx} (T_{wall,node z-1} - T_{wall,node z}) = 0 \text{ eq. 5-1a} \end{aligned}$$

Rearranging eq. 5-1a gives the following:

$$\begin{aligned} -\frac{k_{pipe} A_{pipe}}{dx} T_{wall,node z-1} + \left( \pi D_i dx h_l + \frac{k_{pipe} A_{pipe}}{dx} + \frac{k_{pipe} A_{pipe}}{dx} \right) T_{wall,node z} - \\ \frac{k_{pipe} A_{pipe}}{dx} T_{wall,node z+1} = \pi D_o dx \ddot{Q}_{w,out} + \pi D_i dx h_l T_{ref,node z} \text{ eq. 5-1b} \end{aligned}$$

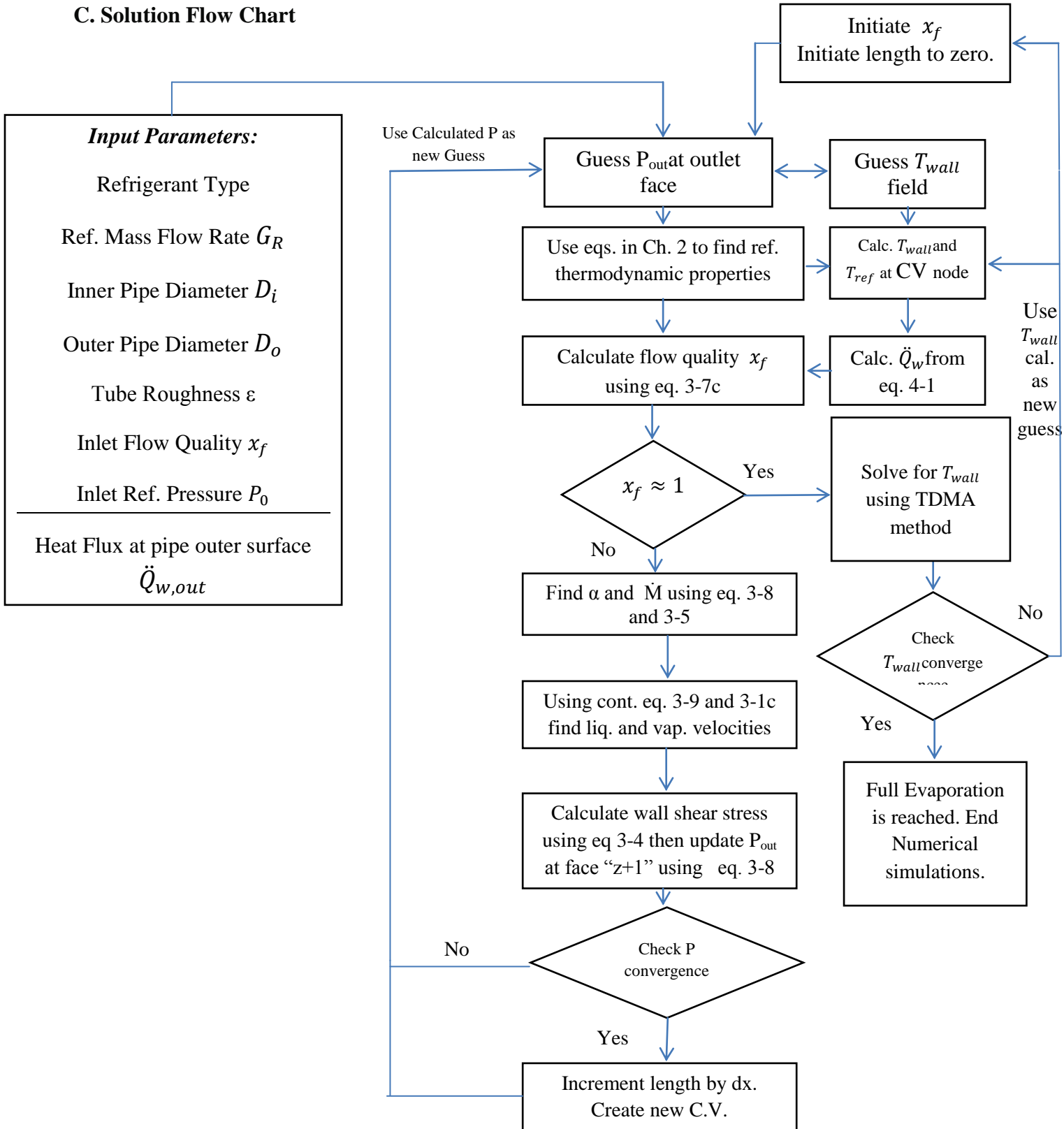
$$-c_z T_{wall,node z-1} + a_z T_{wall,node z} - b_z T_{wall,node z+1} = d_z \text{ eq. 5-1c}$$

Thus a relation between pipe wall temperatures at adjacent control volumes is established. Note that the source term “d” depends on the applied heat and refrigerant temperature at refrigerant control volume z.

Solving for pipe wall temperature using tri diagonal matrix method is straightforward. For more elaboration revise MECH 764 lectures.

The pipe wall temperature field convergence will be checked with the previously guessed field. If convergence is reached, full evaporation is reached and evaporator length is determined. If not, use the TDMA calculated pipe wall temperature field instead of the previously guessed one. Solve for the refrigerant temperature field using equations mentioned in Chapter 3. Use the refrigerant temperature field to update wall pipe temperature field. Iterations will proceed until convergence.

### C. Solution Flow Chart





## D. Results

As mentioned in chapter 3, the base case used from now on will depend on R134a as the refrigerant under study. In order to compare the effect of axial heat conduction through the pipe wall, same conditions for R134a will be used. The only remark is that the heat flux imposed on the outer pipe wall must be the same as the one imposed in chapter 3 in the R134a evaporation case. Thus using *eq. 4-1* and *eq. 4-2* we can deduce that:

$$\ddot{Q}_{w,out} = \ddot{Q}_{w,in} \frac{D_i}{D_o}$$

### R134a Evaporation Process Inputs

$$D_i = 1 \text{ cm}, D_o = 1.27 \text{ cm}, \varepsilon = 1.5 \times 10^{-6}, \quad P_0 = 0.37 \text{ Mpa}, \quad x_f = 0.2,$$

$$\ddot{Q}_{w,out} = 7874 \text{ W/m}^2, \quad \dot{m} = 0.0314 \text{ Kg/s}$$

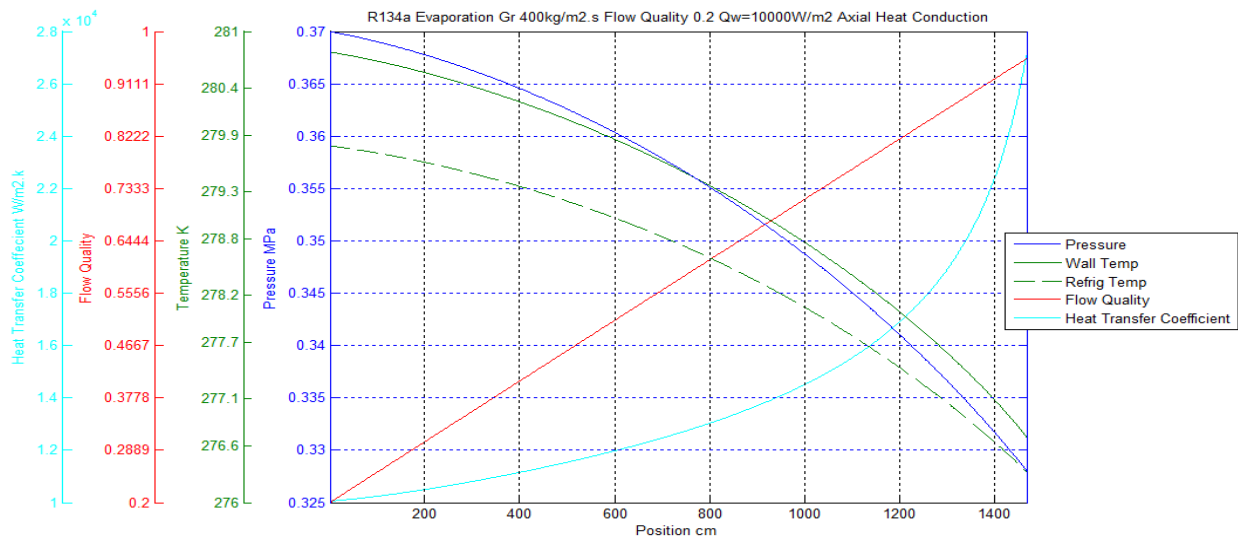


**Figure 19: Variation of pressure, refrigerant and heat exchanger wall temperature, heat transfer coefficient, flow quality, of R134a during evaporation with axial heat conduction taken into consideration**

Notice that in Figure 19 length needed to reach full evaporation is 14.69m while that needed in the same case but without axial heat conduction mentioned earlier in chapter 3 was 15.48m.

Notice also that wall temperature reaches a minimum of 276.7K while in the base case the minimum temperature at the end of the pipe was 276K. Heat transfer coefficient reaches a maximum of  $2.8 \times 10^4$  W/m<sup>2</sup>K compared to  $6 \times 10^4$ .

All of these results show the significance of axial heat conduction in this case where the decrease in length needed which was around 5.1% means the capacity of the evaporator is met with smaller evaporator size. Heat propagating through the pipe wall increased the pipe wall temperature which helped in creating a temperature charge between the pipe and the refrigerant thus leading to more evaporation of the refrigerant.

To make sure the results are consistent, a parametric study on the effect of varying refrigerant mass flow rate on the evaporator length and pipe wall temperature at the end of the pipe in both cases (with axial heat conduction and without) was implemented.

**Table 5: Parametric study showing effect of axial heat conduction on evaporator length during constant heat flux**

$G_R$ kg/m <sup>2</sup> .s	No axial heat conductionLength m	Axial Heat ConductionLength m	Decrease % in length
50	1.94	1.89	2.58
100	3.86	3.72	3.63
200	7.71	7.45	3.37
300	11.58	11.06	4.5
400	15.48	14.69	5.1
600	22.96	21.39	6.84

In table 5, the parametric study shows that as the mass flux of the refrigerant increases the effect of the axial heat conduction becomes more obvious especially on the evaporator length. Thus assuming axial heat conduction helps in predicting the real behaviour of an evaporator.

# CHAPTER VI

## VARIABLE HEAT FLUX - AXIAL HEAT CONDUCTION

### SOLUTION METHODOLOGY & RESULTS

#### A. Mathematical Model

In this chapter, variable heat flux will be applied to the refrigerant wall with axial heat conduction being taken into consideration. A double pipe heat exchanger will be used where the refrigerant passes in the inner tube and water in the outer tube. The inner pipe internal diameter will be denoted by  $D_i$  while the inner pipe outer diameter will be  $D_o$ . The outer pipe internal diameter will be denoted by  $D_s$ . See figure20.

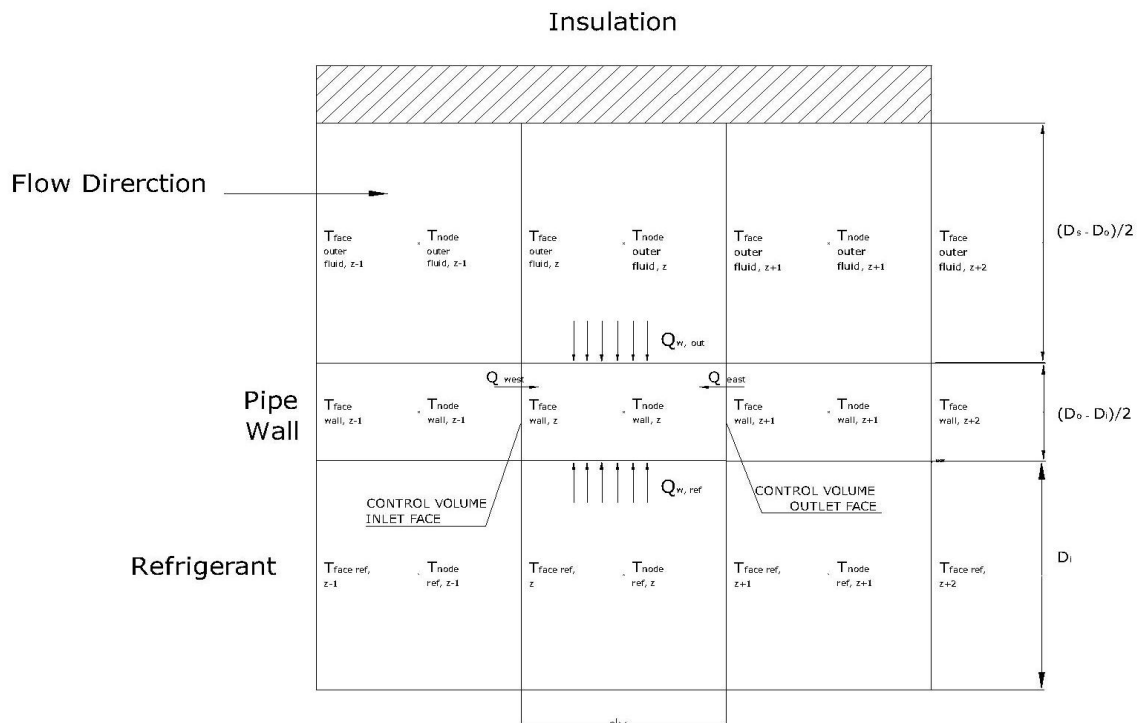


Figure 20: Cross section of concentric pipe

As mentioned in chapter 5, since axial heat conduction is assumed to propagate in the pipe wall, heat flux propagating through the outer wall of the pipe  $\ddot{Q}_{w,out}$  is not totally transferred to the refrigerant. Some of the heat is passing to the surrounding control volumes of the pipe wall. Thus the heat transferred to the refrigerant is the heat input at the outer wall pipe minus the heat transferred to surrounding control volumes.

The problem is that we don't know the quantity of heat passing to the refrigerant, and we know nothing about the pipe wall temperature. We just know the outer fluid mass flux  $G_{of}$  and its inlet temperature  $T_{of,inlet\ face}$ , in addition to refrigerant flow quality  $x_f$ , inlet pressure  $P_0$ , and mass flux  $G_R$ .

## B. Solution Method

Outer fluid temperature field and wall temperature field will be guessed. Pressure at refrigerant control volume outlet face will be guessed. Inner pipe heat flux value  $\ddot{Q}_w$  will be calculated using eq-4.1. Flow quality will be solved using eq. 3-7c. Equations will proceed as in chapter 3 until flow quality is approximately 1.

Outer fluid temperature field is updated using the following equation:

Heat transmitted through outer pipe wall = Heat lost by outer fluid

$$Q_w = h_{out\ fluid} \pi D_o dx (T_{wall,node\ z} - T_{of,node\ z}) = \dot{m}_{out\ fluid} C_{p_{out\ fluid}} (T_{of,face_{z+1}} - T_{of,face_z}) \text{eq. 6-1}$$

Equation 5.1 will be used to solve for updated values of pipe wall which satisfies both equations eq-4.1 and eq-6.1.

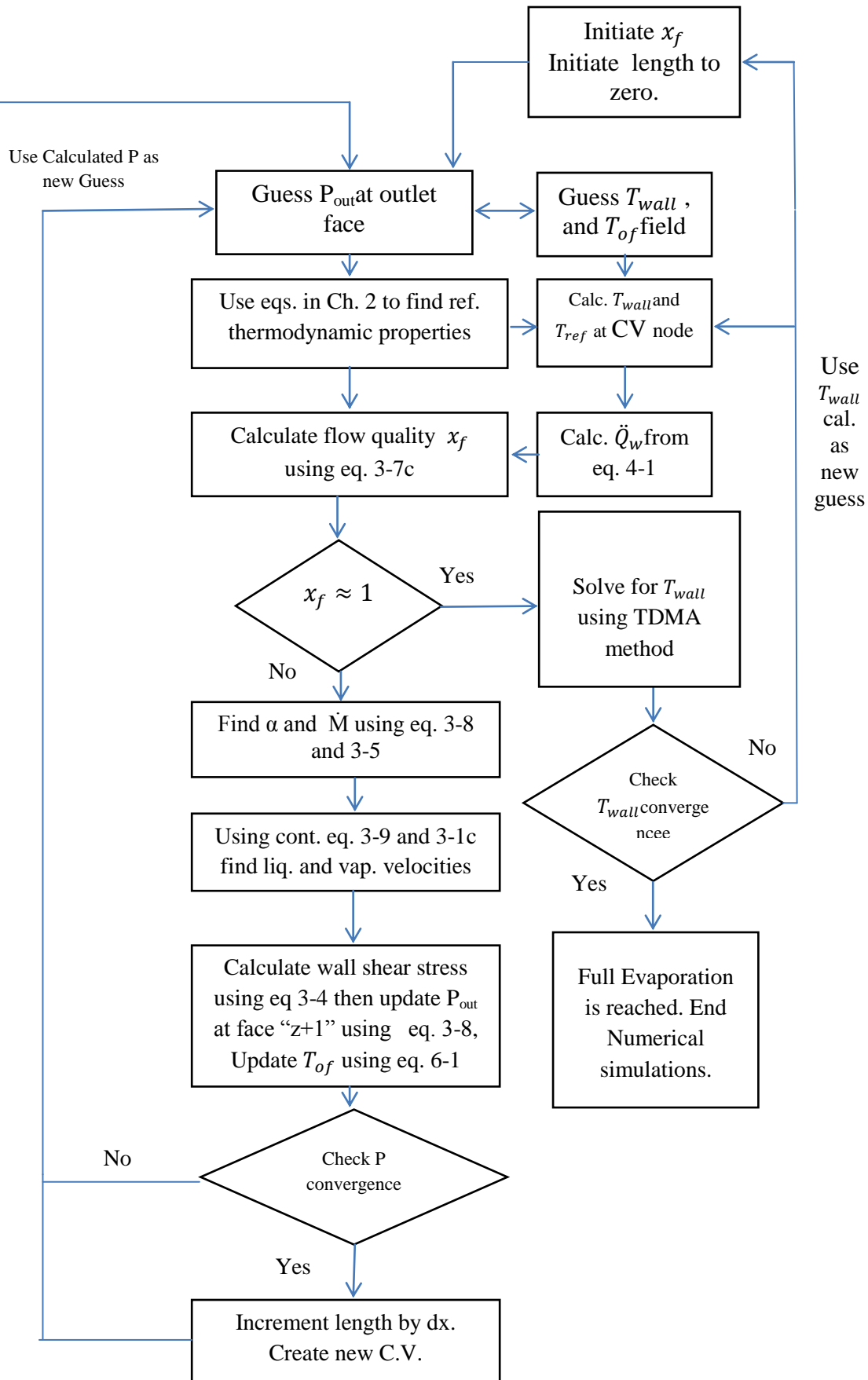
### C. Solution Flow Chart

**Input Parameters:**

- Refrigerant Type
- Ref. Mass Flow Rate  $G_R$
- Inner Pipe Diameter  $D_i$
- Outer Pipe Diameter  $D_o$
- Tube Roughness  $\epsilon$
- Inlet Flow Quality  $x_f$
- Inlet Ref. Pressure  $P_0$

---

- Annulus Diameter
- Outer Fluid Type
- Outer Fluid Mass Flow Rate  $G_{of}$
- Outer Fluid Inlet Temperature  $T_{of,inlet face}$



## D. Results

Same input conditions used in chapter 4 were used.

$$D_i = 1 \text{ cm}, D_o = 1.27 \text{ cm}, \varepsilon = 1.5 \times 10^{-6}, \quad P_0 = 0.37 \text{ Mpa}, \quad x_f = 0.2$$

$$\dot{m}_{ref} = 0.0314 \text{ Kg/s} \text{ or } G_w = 400 \text{ Kg/m}^2\text{s}$$

$$D_s = 2.8 \text{ cm}, \text{Outer Fluid Type: Water, Water Mass Flow Rate } G_w = 114 \text{ Kg/m}^2\text{s}, \text{ Water}$$

$$\text{Inlet Temp. } T_{w,inlet \text{ face}} = 300\text{K}$$

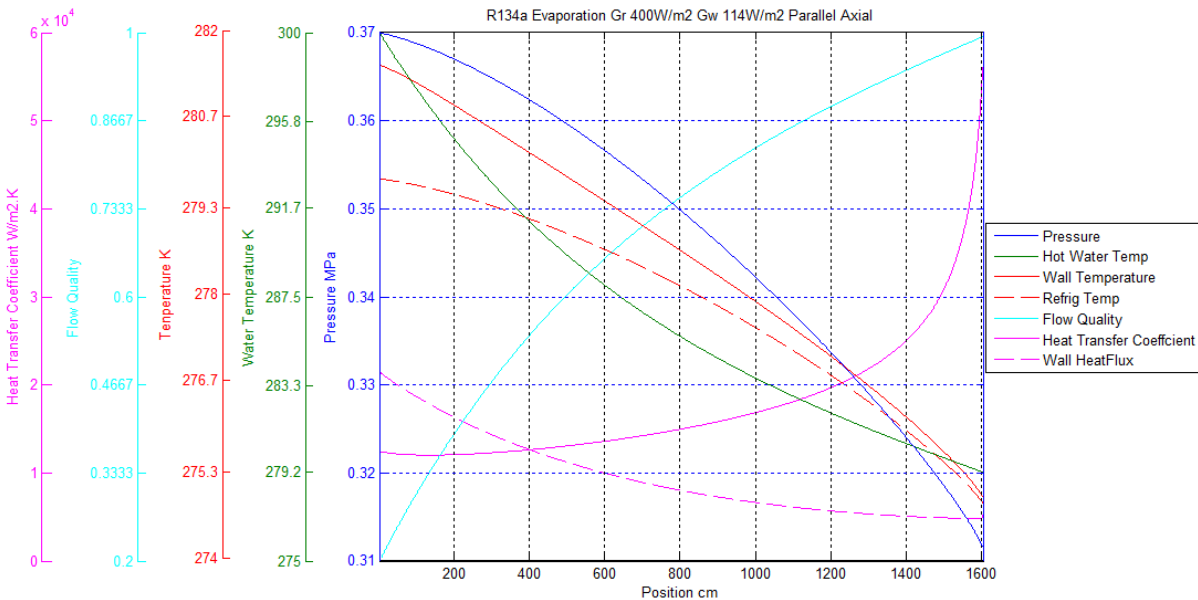


Figure 21: Variation of pressure, refrigerant and heat exchanger wall temperature, heat transfer coefficient, flow quality, of R134a during evaporation with axial heat conduction taken into consideration

Figure 21 shows that the needed length to reach full evaporation is longer than the one needed if axial heat conduction isn't taken into consideration, which means that under sizing of pipe dimensions could occur. This is mainly because of the difference of heat flux and heat transfer coefficient between the two cases whereas the heat flux and the heat transfer coefficient are lower in value in the case where axial heat conduction is taken into consideration.

Table 6 and Table 7 show that as mass flux of refrigerant increases or mass flux of outer fluid decreases (that is decreasing the wall heat flux), the effect of axial heat conduction increases. Unlike results of constant heat flux where ignoring axial heat conduction in pipe could lead to over sizing of pipe dimensions, the effect of under sizing is worse since the remaining refrigerant liquid at the evaporator end could, if summed with other inaccuracies, deteriorate the compressor's performance when it enters the compressor in a refrigeration cycle.

**Table 6: Parametric study showing effect of axial heat conduction when refrigerant mass flux is varied on evaporator length during variable heat flux,  $G_w=114\text{kg/m}^2\text{s}$**

$G_R$ kg/m <sup>2</sup> .s	No axial heat conduction Length m	Axial Heat Conduction Length m	Increase % in length
100	2.22	2.21	-0.45%
200	5.05	5.07	0.4%
300	9.22	9.36	1.52%
400	15.21	16.06	5.59%
500	20.53	22.65	10.33%

**Table 7: Parametric study showing effect of axial heat conduction when water mass flux is varied on evaporator length during variable heat flux,  $G_r=400\text{kg/m}^2\text{s}$**

$G_w$ kg/m <sup>2</sup> .s	No axial heat conduction Length m	Axial Heat Conduction Length m	Increase % in length
214	2.14	2.14	0%
194	6.69	6.77	1.2%
174	7.66	7.79	1.7%
154	9.06	9.26	2.21%
134	11.25	11.63	3.38%
114	15.21	16.06	5.59%

## CHAPTER VII

### PARAMETRIC STUDY

#### A. Effect of Refrigerant Type

Full evaporation of 5 types of refrigerants will be studied. The refrigerants are:

R134a, R12, R22, R32, R145a

Same conditions in chapter 4 will be used.

$D_i = 1 \text{ cm}$ ,  $D_o = 1.27 \text{ cm}$ ,  $\varepsilon = 1.5 \times 10^{-6}$ ,  $T_0 = 279.79\text{K}$ ,  $x_f = 0.2$ ,  $G_{ref} = 350 \text{ Kg/m}^2\text{s}$

$D_s = 2.8 \text{ cm}$ , Outer Fluid Type: Water, Water Mass Flow Rate  $G_w = 114 \text{ Kg/m}^2\text{s}$ ,

Water Inlet Temp.  $T_{w,inlet \text{ face}} = 300\text{K}$

Figure 22 shows that different inlet pressures were used to simulate full evaporation for the 5 different refrigerants. These pressures were chosen in order to have same inlet refrigerant temperature of 279.79K for all refrigerants. In spite different lengths to reach full evaporation were needed, the variation of wall temperature, wall heat flux, heat transfer coefficient, and flow quality of R32 were noticed to be different than those of the other 4 refrigerants.

Length needed for R32 was 115m which is around 10 times that of other refrigerants. Hot water temperature dropped drastically in the first 20m after water gave its heat to the refrigerant where the flow quality reached 0.75. After reaching a temperature of 280.5K the temperature difference between water and R32 becomes small and this decreased the wall heat flux from around



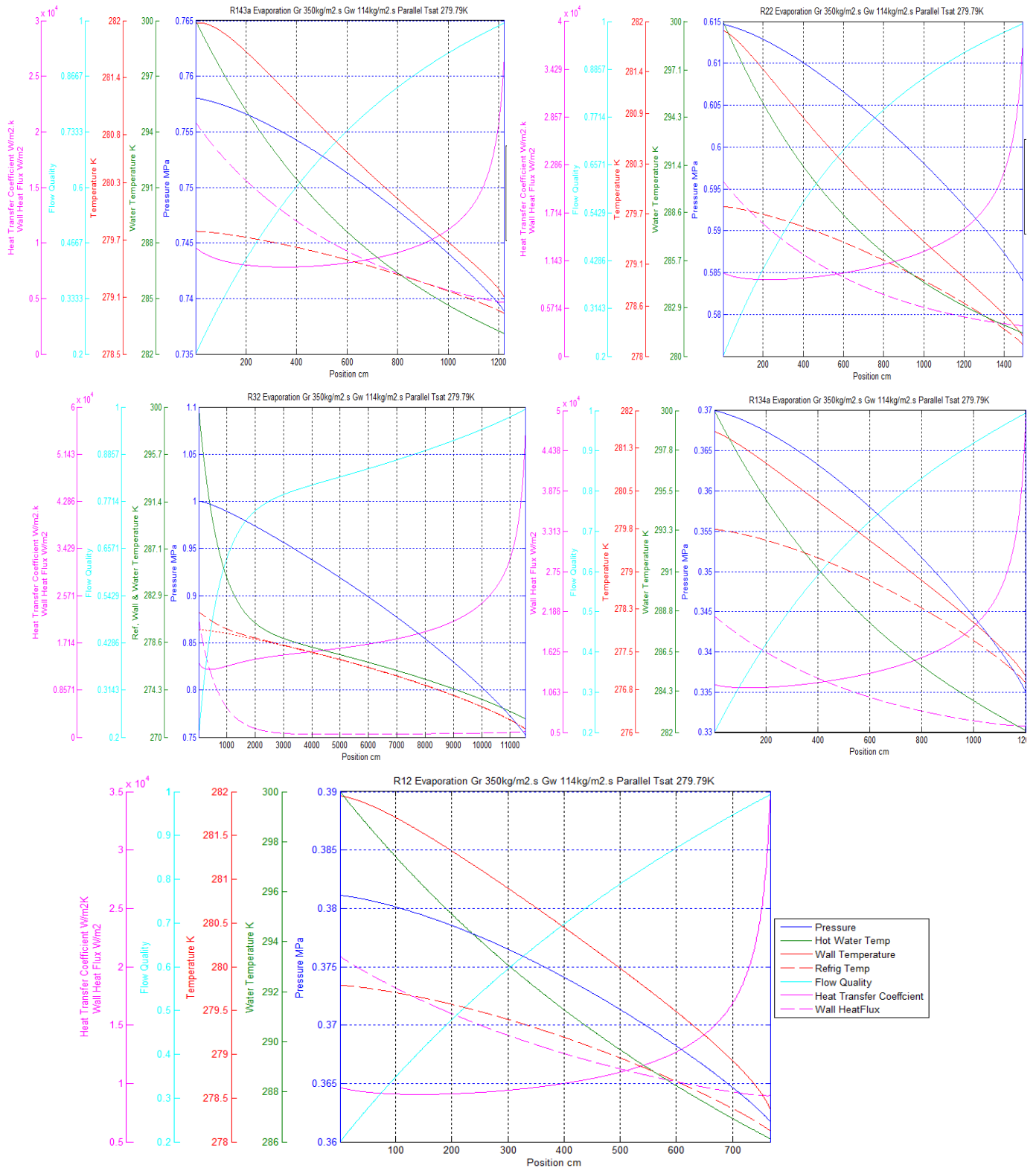


Figure 22: Variation of pressure, refrigerant and heat exchanger wall temperature, heat transfer coefficient, flow quality, during evaporation of R143a, R22, R32, R134a and R12.

21800W/m<sup>2</sup> at pipe beginning to reach 2000W/m<sup>2</sup>. This decrease in wall heat flux slowed down the evaporation process where 95m were needed to evaporate the 25% remaining liquid.

Table 8 shows the length needed for each heat exchanger to fully evaporate the refrigerant mass flux used. The refrigerants were presented according to their latent heat of vaporization from the smallest to the largest. Accordingly the length needed to reach full evaporation was directly related to the latent heat of vaporization. Water temperature drop for both R134a and R143a is approximately equal. Both refrigerants have minor differences in length and average wall heat flux but refrigerant temperature drop is different (2.863K for R134a compared to 0.86K for R143a). This is due to the pressure drop differences where it is around 35kpa for R12 and only 19kPa for R143a. Refrigerant temperature is the saturation temperature of the refrigerant at a corresponding pressure and as pressure decreases its saturation temperature decreases.

**Table 8: Length, average wall heat flux, pressure drop, refrigerant temp drop and water temp drop for R12, R134a, R143a, R22 & R32 respectively with Gr 350kg/m<sup>2</sup>.s**

Refrigerant Type	R12	R134a	R143a	R22	R32
Length (m)	7.69	12.02	12.21	14.91	115.4
% Length of R32 case	6.66%	10.42%	10.58%	12.92%	100%
Average wall heat flux W/m <sup>2</sup>	13450	11060	10270	9267	1824
Pressure Drop kPa	19.41	35	19.12	30	247
Water Temp.Drop K	13.88	17.89	16.88	18.6	28.32
Refrigerant Temp. Drop K	1.666	2.863	0.86	1.643	9.032

[3] proved that during constant heat flux, and when comparing the length variation of different refrigerants, linear variations were noticed since different refrigerants have different latent heat of vaporization. It is clear that length increases as latent heat of vaporization of the refrigerant increases, but in variable heat flux case the difference of length isn't linear. We have noticed the huge difference on length between R32 and the other 4 refrigerants when mass flux of

refrigerants was 350kg/m<sup>2</sup>.s. Another study is performed, with the refrigerant mass flux is taken to be 250kg/m<sup>2</sup>.s, in order to check the length differences between these refrigerants.

**Table 9: Length, average wall heat flux, pressure drop, refrigerant temp drop and water temp drop for R12, R134a, R143a, R22 & R32 respectively with Gr 250kg/m<sup>2</sup>.s**

Refrigerant Type	R12	R134a	R143a	R22	R32
Length (m)	4.82	6.89	6.66	7.62	25.41
% Length of R32 case	18.97%	27.12%	26.21%	29.99%	100%
Average wall heat flux W/m <sup>2</sup>	15350	13880	13470	12990	5948
Pressure Drop kPa	7.46	11.78	6.15	9	29.96
Water Temp.Drop K	9.945	12.86	12.07	13.31	20.35
Refrigerant Temp. Drop K	0.6332	0.9402	0.2749	0.4789	0.9942

Table 9 shows that, when using a mass flux of 250kg/m<sup>2</sup>.s, length needed, when R32 is used, drops from 115m to 25m. The length percentage of each case increased dramatically due to this decrease. As a conclusion, latent heat of vaporization and the variable heat flux applied both have direct effects on the length of heat exchanger used.

### **B. Effect of Variation of Pipe Diameter at Constant Mass Flux**

Input parameters:

$$D_i = 1 \text{ cm} , D_o = 1.27 \text{ cm} , \varepsilon = 1.5 \times 10^{-6} , T_0 = 279.79K , x_f = 0.2,$$

$$G_{ref} = 450Kg/m^2s$$

$$D_s = 2.8 \text{ cm}, \text{Outer Fluid Type: Water, Water Mass Flow Rate } G_w = 114 Kg/m^2s,$$

$$\text{Water Inlet Temp. } T_{w,inlet \text{ face}} = 300K$$

R134a will be used. Inner pipe diameter will be varied from 0.5cm to 1 and 1.5 cm. Mass flow rate will be varied so to have a constant mass flux of 400kg/m<sup>2</sup>.s.

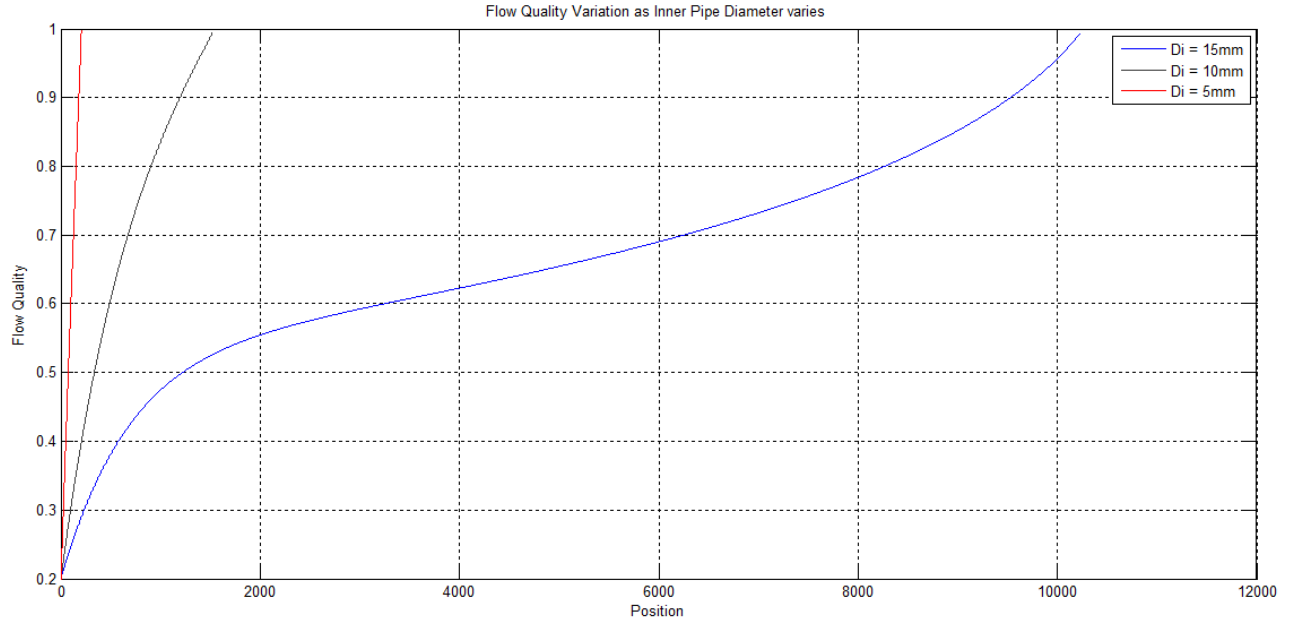


Figure 23: Flow quality variation vs pipe length in the 3 case: Di=5cm, Di=10cm, and Di=15cm

Figure 23 shows that, in addition to pipe length variation where length needed to reach full evaporation varies from 2.05m when Di is 5cm to 15.19m for Di=10cm and at Di=15cm length becomes 102.3m, the flow quality curve doesn't follow the same pattern in varying from 0 to 1, where it is almost a straight line at the smallest diameter to become a curve with one inflection point at the middle when the diameter is 10cm, then to become a curve with two inflection points as shown in the figure. Figure 24 explains this pattern clearly as it shows the direct relation between the wall heat flux, water temperature and the flow quality. As the water temperature decreases, the wall heat flux decreases and thus the flow quality curve slope decreases.

### C. Effect of Outer Fluid Flow Direction

The following Input parameters will be used in this investigation. Two flow directions will be studied, a parallel one and a counter flow one.

$$D_i = 1 \text{ cm} , D_o = 1.27 \text{ cm} , \varepsilon = 1.5 \times 10^{-6} , T_0 = 279.79K , x_f = 0.2,$$

$$G_{ref} = 350 \text{ Kg/m}^2\text{s}$$

$D_s = 2.8 \text{ cm}$ , Outer Fluid Type: Water, Water Mass Flow Rate  $G_w = 114 \text{ Kg/m}^2\text{s}$ ,

Water Inlet Temp.  $T_{w,inlet \text{ face}} = 300\text{K}$

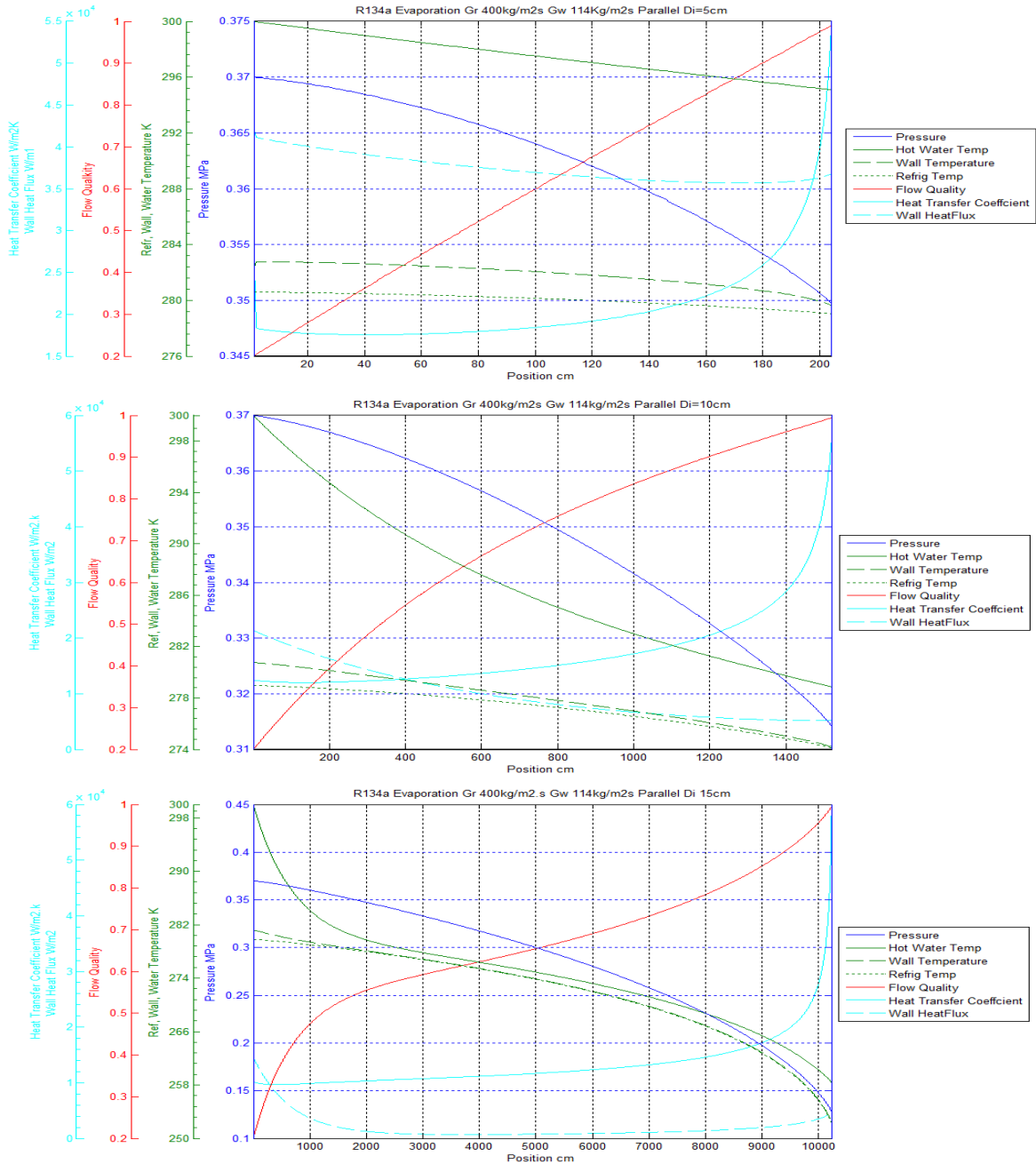
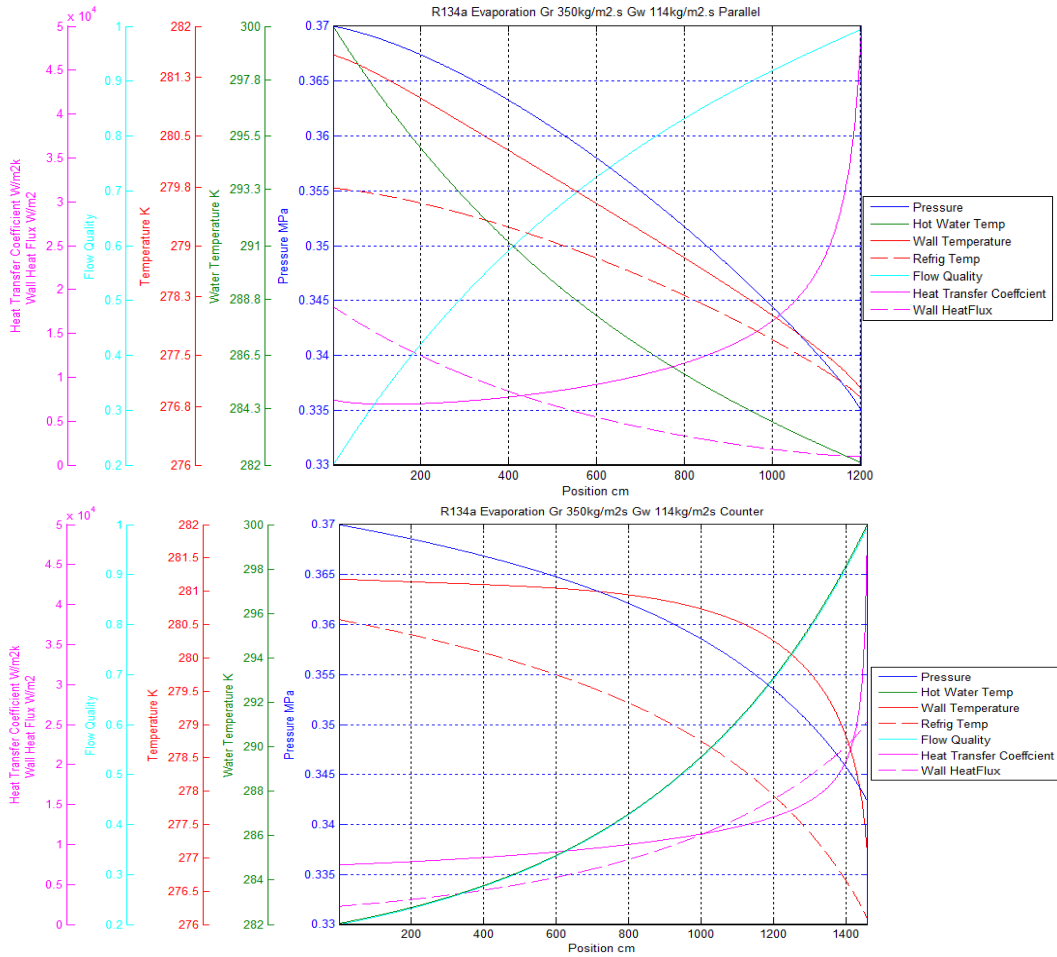


Figure 24: Variation of pressure, refrigerant and heat exchanger wall temperature, heat transfer coefficient, flow quality, during evaporation of R134a for Di=5c, Di=10cm, and Di=15cm.



**Figure 25: Variation of pressure, refrigerant and heat exchanger wall temperature, heat transfer coefficient, flow quality, during evaporation of R134a for parallel flow and counter flow of water**

Figure 25 shows clearly that length needed to reach full evaporation of R134a has increased from 12.02m to more than 14.4m when water flow changed from parallel to counter. This result was based on using 350kg/m2.s of R134a. Decreasing the mass flux to 300kg/m2.s decreases the length difference between the 2 cases to 0.78m (10 m counter, 9.22m parallel). Using a mass flux of 250kg/m2.s leads to a difference of 0.27m (7.18m counter, 6.91m parallel).

The results are due to the difference of wall heat flux at the beginning of the evaporation process. In parallel flow, at steady state the water inlet temperature is around 282 K, 284.5K, and 287K for mass fluxes of 350, 300, and 250 kg/m2.s respectively. The initial temperature difference is

small compared to the parallel flow case which slows the evaporation process, this is clear from the pattern of the flow quality curve where it is clear in figure 24, that at 6m the flow quality of the refrigerant in the parallel flow case is 0.73 while it is 0.35 only in the counter flow case.

$G_R$ kg/m <sup>2</sup> .s	Parallel Flow Length m	Counter Flow Length m	Increase % in length
250	6.91	7.18	3.9%
300	9.22	10	8.46%
350	12.02	14.4	19.8%

## CHAPTER VIII

### CONCLUSION & FUTURE WORK

The current study presented a numerical model for solving two-phase flow of refrigerants subjected to constant or variable heat flux. Surely it was noticed that the dynamics change as the heat flux varies. Flow quality curve diverted from a linear one to a curve that changes its slope depending on the heat flux applied. Evaporator or condenser size changed as mass flux of refrigerant or mass flux annulus fluid changed.

Latent heat of vaporization of different refrigerants, combined with the variation of the wall heat flux, affected the length needed to reach full evaporation. This change doesn't follow a predicted pattern and length percentages of different refrigerants varied when mass flux changed.

Axial heat conduction effect was studied. It was shown that neglecting axial heat conduction, when constant heat flux is applied, could oversize the evaporator length (depends on the mass flux and heat flux applied). On the other hand, neglecting it could undersize the evaporator length if variable heat flux is applied.

Pipe size diameter was varied, with keeping constant mass flux, and it had great impact on the evaporator length. Flow direction was investigated where counter flow of outer fluid opposed to the refrigerant had negative impact on the length needed to reach full evaporation.

Many assumptions were taken into considerations and for more reliable results any future work must take them into consideration. In our study, annular flow was assumed while other flow types should be addressed. Heat transfer coefficient of the outer fluid didn't take into consideration the change of the outer fluid temperature. Thermal conductivity of the pipe was



considered constant and in order to assess the real contribution of axial heat conduction its explicit relation with other variables (temperature) must be used. Wall temperature variation was considered only in axial direction neglecting its change in the radial direction. Gravitational effects weren't studied....

Finally, use of newer refrigerants in any future work is a must. New refrigerants thermodynamic properties must be studied to allow for the use of such refrigerants in older air conditioning and refrigeration systems. Performance of these refrigerants could be simulated before their application in the industry.

## REFERENCES

[1] S. Bendapudi, and J.E. Braun, (2002), "A review of literature on dynamic models of vapor compression equipment", ASHRAE 1043-RP, TC 4.11.

- [2] B.P. Rasmussen, (2012), “Dynamic modeling of vapor compression systems – Part I: Literature review”, HVAC Res. 18 (5) (2012) 934–955.
- [3] I. Fayssal& F. Moukalled, (2012), “A New Numerical Approach for Predicting the Two Phase Flow of Refrigerants during Evaporation and Condensation”, Numerical Heat Transfer, Part B: Fundamentals, 62:5, 341-369, DOI: 10.1080/10407790.2012.707009.
- [4] M. Y. Lee, (2017), “Design and Cooling Performances of an Air Conditioning System with Two Parallel Refrigeration Cycles for a Special Purpose Vehicle”, Appl. Sci. 2017, 7, 190; doi:10.3390/app7020190 .
- [5] N. Rachapradit, S. Thepa, and V. Monyakulb, (2012), “An Influence of Air Volume Flow Rate and Temperature Set Point on Performance of Inverter Split-Type Air-Conditioner”, Experimental Techniques 36 (2012) 18–25 © 2011, Society for Experimental Mechanics.
- [6] D. Parker, J. Sherwin, R. Raustad, and D. Shirey, (1997), “Impact of Evaporator Coil Airflow in Residential Air-Conditioning Systems”, III ASHRAE Transactions; 1997; 103, ProQuest Central pg. 395.
- [7] A. Ebrahimi-Mamaghani, R. Sotudeh-Gharebagh, R. Zarghami, and N. Mostoufi, (2019), “Dynamics of two-phase flow in vertical pipes”, Journal of Fluids and Structures 87 (2019) 150–173.
- [8] Z. Baniamerian, R. Mehdipour and C. Aghanajafi, (2012), “Analytical Simulation of Annular Two-Phase Flow Considering the Four Involved Mass Transfers”, August 2012, Vol. 134 / 081301-1.

- [9] T. Okawa, T. Goto, and Y. Yamagoe, (2009), “Liquid film behavior in annular two-phase flow under flow oscillation conditions”, *International Journal of Heat and Mass Transfer* 53 (2010) 962–971.
- [10] E.N. Sieder, G.E. Tate, (1936), “ Heat transfer and pressure drop of liquids in tubes”, *Ind. Eng. Chem.* 28 (1936) 1429–1435.
- [11] S. Whitaker, (1972), “Forced Convection Heat Transfer Correlations for Flow In Pipes, Past Flat Plates, Single Cylinders, Single Spheres, and for Flow In Packed Beds and Tube Bundles”, *AIChE Journal* (Vol. 18, No.2) p361.
- [12] V. Gnielinski, (1975), "Neue Gleichungen für den Wärme- und den Stoffübergang in turbulent durchströmten Rohren und Kanälen", *Forsch. Ing.-Wes.* 41 (1): 8–16.
- [13] I. Tosun, (2007), “Modeling in Transport Phenomena (Second Edition) A Conceptual Approach”, Pages 59-115.
- [14] F.W. Dittus, and L.M.K. Boelter, (1930), *University of California Publications on Engineering*, Vol. 2, p. 443, Berkeley.
- [15] A. Zhukauskas, (1972), “Advances in Heat Transfer, Vol. 8: Heat Transfer From Tubes in Cross Flow”, Eds. J.P. Hartnett and T.F. Irvine, Jr., Academic Press, New York.
- [16] S.W. Churchill, and M. Bernstein, (1977), “A correlating equation for forced convection from gases and liquids to a circular cylinder in cross flow”, *J. Heat Transfer*, 99, 300.
- [17] S. Marathe, and R. Webb, (2007), “Prediction of dryout vapor quality for annular two-phase flow in tubes”, *Applied Thermal Engineering* 28 (2008) 691–698.

- [18] Z. Baniamerian, and C. Aghanajafi, (2010).“Studying the influence of refrigerant type on thermal efficiency of annular two-phase flows; mass transfer viewpoint”, Korean J. Chem. Eng., 28(1), 49-55 (2011).
- [19] S. Wongwises, S. Disawas, J. Kaewon, and C. Onurai, (2000), “Two-phase evaporative heat transfer coefficients of refrigerant HFC-134a under forced flow conditions in a small horizontal tube”, Int. Comm. Heat Mass Transfer, Vol. 27, No. 1, pp. 35-48, 2000.
- [20] W. Sripattrapan, S. Wongwises, (2005), “Two-phase flow of refrigerants during evaporation under constant heat flux in a horizontal tube”, International Communications in Heat and Mass Transfer 32 pp 386 – pp 402.
- [21] J. Ahn, E.M. Sparrow, J.M. Gorman, (2017), “Turbulence intensity effects on heat transfer and fluid-flow for a circular cylinder in crossflow”, International Journal of Heat and Mass Transfer 113 (2017) 613–621.
- [22] N. Kattan, J. R. Thome, D. Favrat, (1998), “Flow Boiling in Horizontal Tubes: Part 3—Development of a New Heat Transfer Model Based on Flow Pattern”, Transactions of the ASME, Vol. 120, February 1998.
- [23] F. Moukalled , J. Kasamani, S. Acharya (1992),“Turbulent Convection Heat Transfer in Longitudinally Conducting, Externally Finned Pipes”, Numerical Heat Transfer, 21:4, 401-421, DOI: 10.1080/10407789208944884.
- [24] G. Maranzana, I. Perry, D.Maillet (2003), “Mini- and micro-channels: influence of axial conduction in the walls”, International Journal of Heat and Mass Transfer 47 (2004) 3993–4004.

- [25] G.P. Celata, “Single and Two-Phase Flow Heat Transfer in Micropipes”, 5th European Thermal-Sciences Conference, The Netherlands, 2008.
- [26] Table 2.14, (2017), “Lifetimes, radiative efficiencies and direct (except for CH<sub>4</sub>) GWPs relative to CO<sub>2</sub>”, IPCC Fourth Assessment Report: Climate Change 2007, [http://www.ipcc.ch/publications\\_and\\_data/ar4/wg1/en/errataserrata-errata.html](http://www.ipcc.ch/publications_and_data/ar4/wg1/en/errataserrata-errata.html) .
- [27] Directive 2006/40/EC of the European Parliament and of the council of 17 May 2006 relating to emissions from air-conditioning systems in motor vehicles and amending Council Directive 70/156/EEC
- [28] T. Mahajani and P. Lokhande, (2018), “Review of Current Automobile Refrigeration System on Basis of Refrigerants Used & Their Impact on Global Warming Potential”, IOSR Journal of Mechanical and Civil Engineering (IOSR-JMCE) e-ISSN: 2278-1684,p-ISSN: 2320 334X PP. 82-87
- [29] R. Tillner-Roth and H. Baehr , (1994), “An International Standard Formulation for the Thermodynamic Properties of 1,1,1,2-Tetrafluoroethane (HFC-134a) for Temperatures from 170 K to 455 K and Pressures up to 70 MPa”, Journal of Physical and Chemical Reference Data 23, 657.
- [30] M.L. Huber, A. Laesecke, and R.A. Perkins, (2003), “Model for the Viscosity and Thermal Conductivity of Refrigerants, Including a New Correlation for the Viscosity of R134a”, Ind. Eng. Chem. Res., 42:3163-3178, 2003.
- [31] R.A. Perkins, A. Laesecke, J. Howley, M.L.V. Ramires, A.N. Gurova, and L. Cusco, (2000), “Experimental thermal conductivity values for the IUPAC round-robin sample of 1,1,1,2-tetrafluoroethane (R134a)”, NISTIR, 2000.

[32] M. McLinden, S. Klein, R. Perkins, (1999), "An extended corresponding states model for the thermal conductivity of refrigerants and refrigerant mixtures", *International Journal of Refrigeration* 23 (2000) 43-63.

[33] A. Mulero, I. Cachadiña, M. I. Parra, (2012), "Recommended Correlations for the Surface Tension of Common Fluids", *J. Phys. Chem. Ref. Data* 41, 043105 (2012); <https://doi.org/10.1063/1.4768782>.

[34] M. Okada and Y. Higashi, (1994), "Surface tension correlation of HFC-134a and HCFC-123", CFCs, The Day After (Proceedings of the Joint Meeting of IIR Commissions B1, B2, E1, and E2), Padua, Italy, 541-548, 1994.

[35] M. Awad, (2012), "Two-Phase Flow", Intech open, An Overview of Heat Transfer Phenomena, Chapter 11.